

8/16/91

FINAL REPORT  
EXPERIMENTAL VERIFICATION OF A NEW LAMINAR AIRFOIL  
A PROJECT FOR THE GRADUATE PROGRAM IN AERONAUTICS

By

Mr. Oran W. Nicks  
Co-Principal Investigator  
&  
Dr. Kenneth D. Korkan  
Co-Principal Investigator

Texas A&M University  
Aerospace Engineering Department

*1/10/91*  
*10/2/91*  
*37752*  
*P.41*

A student project involving two Masters' students and three Seniors has been completed in accordance with a NASA Grant No. NAG-1-1260. This is a final report concerning this project. The NASA contribution to the project covered costs of materials for fabricating the model and travel to the conference. The Texas A&M University contribution provided a basic model suitable for modification and the wind tunnel testing period of approximately 40 hours occupancy time. The co-principal investigators and the students performed the tasks on a time available basis making the project a three-way cooperative experience.

The students performed the work in two teams, one performing experimental research under the supervision of Mr. Nicks and the other conducting analytical investigations under Prof. Korkan. The two teams worked together to coordinate all phases of the activities and shared in the testing and analyses plus the formal presentation of two papers at an international conference, the XXII OSTIV Congress held in conjunction with the World Championship Soaring Competition. Copies of the papers are included and will be published in the official OSTIV Congress publication and in Technical Soaring, a refereed journal having wide distribution to an international audience.

The students obtained benefits from direct association with Mr. Dan M. Somers and Prof. Mark D. Maughmer, designers of the SM701 Airfoil. These two professionals

(NAG-1-1260) EXPERIMENTAL VERIFICATION  
OF A NEW LAMINAR AIRFOIL: A PROJECT FOR THE  
GRADUATE PROGRAM IN AERONAUTICS Final Report  
(TEXAS A&M UNIV.) 8/16/91

91-10092

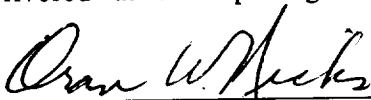
Unclass

05/02 0037199

provided tutoring for the students on the use of the airfoil design program and offered consultation during the experimental tests and analyses.

The student experience involved a combination of analytical design, hands-on model fabrication, wind tunnel calibration and testing, data acquisition and analysis, comparisons of test results and theory, and the preparation and presentation of papers at an international conference. This spectrum of activities afforded experience and insight concerning the conditions necessary for achieving and maintaining natural laminar flow and the importance of airfoil design and performance in the real-world operating environment. A summary presenting the viewpoint of the student team is attached along with copies of the two papers and a keynote address delivered at the opening of the Congress.

Signatures:

  
\_\_\_\_\_  
Mr. Oran W. Nicks

  
\_\_\_\_\_  
Dr. Kenneth D. Korkan

Enclosures:

Soaring Technology Advances--Challenges and Opportunities  
Wind Tunnel Investigation and Analysis of the SM701 Airfoil  
Verification of the SM701 Airfoil Aerodynamic Characteristics Utilizing  
Theoretical Techniques  
Student Team Comments

## STUDENT TEAM COMMENTS

We would like to take this opportunity to make some personal comments on the experience made possible through the grant NAG-1260-FDP. The initial obvious benefit was being able to organize and run a wind tunnel test from start to finish. We designed and built the model to be tested, planned the test matrix, performed the experiments, analyzed the data, wrote the final report, and presented the results at the XXII OSTIV Conference. This is a big addition to the usual experience of simply collecting data for another user.

Throughout the course of the project, the model construction provided the greatest learning experience. We had very little previous exposure to the foam and fiberglass construction techniques employed. By the time the model was completed however, we had become very competent with the techniques required, as well as every inch of the model. We worked the approximately 42 ft<sup>2</sup> of surface area by hand to the final finish.

Planning the test matrix afforded the opportunity of learning the trade-offs required to balance time available, data desired, and schedules of people.

The actual running of the test had two significant highlights for us. The first was seeing our work on the model and the test preparation pay off. The second was the chance to meet and learn from Mr. Dan Somers of Airfoils, Inc. and Dr. Mark Maughmer of Penn State University. The running of the test also provided numerous learning opportunities. We spent significant amounts of time trying to understand and eliminate or correct for the three-dimensional and tunnel boundary layer effects present on our two-dimensional airfoil section.

The most exciting time in the project came near the end. The preparation for and attendance at the XXII OSTIV Conference along with the World Gliding Championships was a once in a lifetime experience. We had the chance to present

our test results and conclusions to a large group of international scientists and engineers through both an oral presentation and the eventual publication of our paper in Technical Soaring. In addition to this, we met a number of very famous people who have become familiar to us through textbooks and magazine articles, but we never expected to get to talk personally or eat dinner with them. On a practical level, none of us had ever been exposed to soaring or gliders prior to this project. While attending the OSTIV Conference, we not only got to see these beautiful ships fly competitively, but were shown and allowed to feel their unique characteristics by many of their designers.

In conclusion, we cannot say enough about the incredible experience this entire project has been for all of us. We truly feel it has been a once in a lifetime chance. We would like to convey our deepest gratitude to all the people at NASA Langley Research Center whose support helped make this all possible.

SIGNED:

  
\_\_\_\_\_  
David Bauer  
\_\_\_\_\_  
Mike Heffner  
\_\_\_\_\_  
Greg Steen

## SOARING TECHNOLOGY ADVANCES--CHALLENGES AND OPPORTUNITIES

Keynote Address - OSTIV Opening Ceremony, August 1, 1991

Oran W. Nicks

### Introduction

This conference brings together creative scientists, engineers, craftsmen, and pilots from around the globe. While the World Soaring Championships are underway, our OSTIV Congress will discuss science and technology that will affect future World Championships. Many in this room have been directly responsible for the advances which have allowed this sport to evolve into the sophisticated activity that it has become.

It is therefore fitting that as we hear of new discoveries and see current equipment and users in action that we take the greatest advantage of this opportunity. Through the sharing of information, we are able to assimilate and integrate ideas, theories and findings as we direct our attention to our possible contributions in the future.

As counterparts of these Championship pilots, we carry a responsibility for the quality of their equipment, for their understanding of the natural environment and for the application of the science and technology in the sport. I, therefore, encourage you to listen intently throughout the conference, to concentrate on the information that is presented and do your best to overcome the barriers of language, background, competitiveness, or temperament that might in anyway reduce the effectiveness of this opportunity to share and to learn.

To prepare for this conference I reviewed major factors involved in soaring and made a list of ideas that I believe offer promise for advances in them. Some of these ideas have been researched and tried before without success. From my long list, I have selected four areas for discussion, where I believe significant challenges and opportunities exist.

### COST

The first of these is COST, and my reason for putting this first is that I believe our sport can become much more than it is if sailplanes can be less expensive. More people throughout the world could participate in the sport, and more participation would mean more evolution in the science and technology as a result of the greater activity. The cost of our current sailplanes is strongly related to their size, that is, to mass and surface area.

The combination of material costs and labor involved in manufacture are the primary parameters that drive the cost. Most materials are sold by the pound or kilogram or by the square yard or meter. The labor hours involved in manufacture and finishing of current sailplanes is directly proportional to the square meters of surface area, and this increases at over twice the rate as increases in wing area which is proportional to the mass.

During the earliest days of aeronautical design, structural weight was of critical importance. Materials with the best strength to weight ratio were key to this design discipline. Because we have been able to produce sailplanes that can stay up and fly fast carrying extra weight in the form of water ballast, reducing weight has received less emphasis during the past 20 years. Most of the structural evolution has been driven by aerodynamic requirements for thin wings and laminar flow quality surfaces which do not twist under varying conditions. Perhaps as a result of the many successful designs with spans of 15 meters and more, and perhaps because of Standard and 15-meter classes

prescribed for competitions, there has not been much emphasis on considering designs with less than 15 meter spans. This thinking has recently been affected by the World Class Competition, although smaller sailplanes are yet to be seen.

Nevertheless, smaller gliders would not only cost less but would pay dividends in other ways. The friction drag which is so important to gliding is directly proportional to the surface area. The crew strength requirements for assembly would be less, the size of trailers to transport the sailplanes would be less, the automobile towing requirements would be less and the storage requirements would be reduced.

As a young aeronautical engineer during World War II, I vividly recall a placard in the drafting room saying "Simplicate and add lightness", and yet another admonition asking, "Have you saved your ounce today?" The implications were, of course, that mass was important, for in the simplest sense, an ounce of airframe competed with an ounce of payload.

Manpowered aircraft and ultralights have been forced to explore new material applications, and have produced technology allowing extremely light airframes. For those who have examined the successful new kit designs of two and four place general aviation aircraft, the most astonishing difference between them and production designs is overall size. The Lancair and Glasair models, for example, are remarkably smaller than their production counterparts, and they use natural laminar flow and many of the materials technologies employed in sailplanes. I believe we should accept the challenge of designing efficient single place sailplanes with a structures mass fraction of 40% of the gross weight.

## SAFETY

The safest sailplanes are those having good airworthiness, that is, good flying characteristics such as gentle stall, easy handling and maneuverability with predictable, forgiving qualities. The stall speed equates to the minimum speed on landing and since the energy at touchdown is proportional to the square of the velocity, this design parameter is very important. Other obvious features important to the safety of sailplanes include the positive hookup of controls and provision for securing equipment and loose items that prevents barographs or batteries, for example, from becoming lethal missiles during a crash. I am pleased to say that considerations of this sort are becoming much better recognized, partly because of the actions of the OSTIV Sailplane Development Panel and other groups.

Crashworthiness is also being factored into the design process and must continue to be a high priority item. The idea is that structures necessary to support the airworthiness can also be effective during crashes, providing energy absorption after primary failures have occurred. It has been said that the inevitable inevitably happens. When it does, the engineer who has used his professional skills to account for it in a cost-effective manner, has better served mankind than those who looked away from that unpleasant circumstance..

What I would like to advocate as a challenge and opportunity is an interdisciplinary effort to marry new parachute technologies with glider design. The idea has been made obvious by the ultralight movement wherein rescue parachute systems are being attached to these aircraft, allowing both the pilot and his plane to be supported during descent. New parachutes have glide ratios almost as good as early hanggliders, and when coupled with new sailplane crashworthiness techniques, could surely increase safety.



Integral parachutes would offer obvious advantages for club ships and for trainers, where parachute safety could exist with rotation of pilots, many without much emergency bailout training. Cockpit seats and restraints might be improved if the parachutes, most of which do not make very comfortable cushions, were located behind the cockpit out of sight. Their ease of operation, the time saved during emergency deployment, and the benefits to the pilot remaining within the sailplane structure during parachute descent, are potential benefits. From discussions I have had with parachute designers, it appears that costs, masses, and reliability may be competitive for current sailplanes, and certainly could be developed for new designs.

#### PERFORMANCE

Increasing the lift and reducing the drag are the basic aerodynamic performance challenges for gliding flight. The most significant aerodynamic aspect of soaring is our ability to use knowledge of laminar flow principles to lower the skin friction drag of sailplanes. The discovery of different regimes for fluid flows along surfaces and the effects on friction, eventually led to understanding the benefit of laminar flow for lowering drag, and its practical application to sailplanes. Even though laminar flow airfoils were successfully developed and used during World War II, a great amount of skepticism existed for many years among the aviation community, and this skepticism has held back progress. As successful beneficiaries of our understanding of laminar flow, one might think sailplane technologists would pursue the refinements possible with great enthusiasm, yet I sense a tendency to be satisfied with achieving laminar flow over 60-80% of the wing surfaces as about all we can expect. This is not true, and there is a great opportunity to achieve higher percentages of laminar flow. We must not rest until we have come much closer

to 100% laminar flow and realized the additional reduction in drag that is theoretically possible.

### SCIENCE

The atmosphere in which we fly, and the energy to soar provided by solar heating and other natural phenomena, have gradually become known to us by the work of scientists. Soaring pilots apply this knowledge every day, and accumulate additional information each time we fly. Knowledge of pressure gradients, temperatures, densities, gust conditions and turbulence now taken for granted was provided by scientists who discovered and characterized the atmosphere for designers and pilots. Some may conclude that all we need to know has been learned, but that is not the case. Furthermore, soaring pilots, because of our interest in and frequent exposure to the atmospheric environment, are in a position to provide considerably more knowledge of the atmosphere. It was high altitude wave flights after World War II that provided much stimulus and knowledge for large scale effects in the atmosphere. Today our total energy sensors and knowledge of small scale effects have enhanced the understanding of windshear and other influences important to every aspect of flight.

But we can do more. Our recording barographs, our computers capable of storing data about each flight, coupled with our more than layman's knowledge of the atmosphere, allow us the opportunity to contribute basic information for the greater cause. Just imagine how much accumulative data about the atmosphere in Texas will be amassed in the heads of the competition pilots during this contest. Wouldn't it be impressive and useful if these data could be compared, collated and stored for reference. I challenge all of you to consider the contribution you might make to your local soaring community if

you would but take some time to record and share information in a form that is not lost with your fading memories.

### SUMMARY

One of the most exciting aspects of our sport is that we engage in the evolution of technologies, in the understanding and application of our knowledge of the natural environment and in the hands-on aspect of piloting which blends these capabilities. As we gain experience, our opportunities to learn and contribute broaden. I believe this Congress offers the epitome of opportunity for blending these qualities and for savoring the nectar of our sport.

Unfortunately, the basis of progress is not only related to the status of science and technology, but to the attitudes of men. Sir Francis Bacon ably put it this way:

*"By far the greatest obstacle to the progress of science and other undertaking of new tasks and provinces therein, is found in this -- that men despair and think things impossible".*

It is exciting to live in this time of opportunity. It is thrilling to share with friends and colleagues in making the advances that will become evident tomorrow. We must not despair and think things impossible, for there is much more we can do. I hope that you will find this OSTIV Congress a source of new inspiration. Thank you.

**WIND TUNNEL INVESTIGATION AND ANALYSIS  
OF THE SM701 AIRFOIL**

Presented at the XXII OSTIV Congress,  
Uvalde, Texas 1991

NASA Grant Number:  
NAG1-1260-FDP

By:

Oran Nicks  
Gregory Steen  
Michael Heffner  
David Bauer

Low Speed Wind Tunnel  
Texas A&M University  
17 - FM 2347  
College Station, Texas 77840

July 1991

Texas A&M University  
Low Speed Wind Tunnel

**WIND TUNNEL INVESTIGATION AND ANALYSIS  
OF THE SM701 AIRFOIL**

By:

Oran Nicks, Research Engineer

Gregory Steen, Research Specialist

Michael Heffner, CO-OP Student Research Aide

David Bauer, CO-OP Student Research Aide

**ABSTRACT:**

A wind tunnel test was performed on a two-dimensional model of the SM701 airfoil designed for use on World Class gliders. The test covered a range of Reynolds Number conditions from one million to 2.5 million. Aerodynamic forces and moments were measured with an external balance. Wake-rake measurements of the two-dimensional drag were also made. Flow visualization techniques provided information on transition from laminar to turbulent flow. Post stall conditions were examined for both positive and negative angles of attack. Lift, drag, and pitching moment were analyzed and comparisons made with numerical predictions. The model was designed, constructed, and the test conducted by students at Texas A&M University.

Hz	Hertz
kPa	kiloPascals
KVA	kilovolt-amps
lbs	pounds
m	meters
mm	millimeters
N	Newtons
Pa	Pascals
psf	pounds per square foot
RN	Reynolds Number
RPM	revolutions per minute
X	longitudinal distance from test section center
Y	lateral distance from test section center
Z	vertical distance from test section center

**SYMBOLS:**

AR	aspect ratio
$C_{Di}$	induced drag
$C_f$	friction coefficient
$C_L$	lift coefficient
$C_{Lmax}$	maximum lift coefficient
ft	feet

**CONVERSIONS:**

1 inch	= 25.4 millimeters
1 pound force	= 4.448 Newtons
1 foot	= 0.3048 meters
1 psf	= 47.88 Pascals

## BACKGROUND:

The International Gliding Commission (IGC) of the Federation Aeronautique Internationale (FAI) initiated a design and prototype competition in the later part of 1989 for a new World Class glider to be used in international competition. Technical Specifications for this design and ground rules concerning the competition were announced worldwide by the FAI. The specifications were prepared after much deliberation by an international panel incorporating judgements that favor low cost, safety, suitable performance, and ease of handling that might encourage soaring on a worldwide basis.

The balanced characteristics chosen by the panel suggested the desirability of a high maximum lift coefficient, gentle stall and adequate L/D ratios at low Reynolds Numbers. Two experienced airfoil designers, Mr. Dan M. Somers and Dr. Mark D. Maughmer teamed to design a suitable airfoil, taking into account the compromises involved in World Class Technical Specifications. The SM701 airfoil was designed using the Eppler-Somers Airfoil Design Program. Its physical and design characteristics were then offered to all designers who might wish to employ this new section.

Because the analytical procedures are limited in the determination of some parameters such as maximum lift coefficient, characteristics after stall, determination of zero lift angle of attack, and pitching moment, it was proposed that experimental tests be conducted on a two-dimensional model of the SM701. A student project proposed by Texas A&M University was funded by NASA to perform this test using a modified wind tunnel model. The test was conducted and this report was prepared by a student team and an advisor at Texas A&M University under NASA Grant Number NAG1-1260-FDP. Mr. Dan Somers and Dr. Mark Maughmer provided consultation during the test along with lectures on the application of the Eppler-Somers airfoil design method.

## FACILITY DESCRIPTION:

The Texas A&M University Low Speed Wind Tunnel (TAMU-LSWT) is a self contained research facility located adjacent to Easterwood Airport in College Station, Texas.

The wind tunnel is of the closed circuit, single return type having a rectangular test section ten feet wide and seven feet high. Figure 1 presents a line drawing of the second floor of the building and a plan view of the wind tunnel circuit. Total circuit length at the centerline is 396 feet (120.7 m). The maximum diameter of 30 feet (9.14 m) occurs in the settling chamber. A single screen is located at the settling chamber entrance and a double screen just upstream of the contraction section to improve dynamic pressure uniformity and to reduce flow turbulence levels.

The contraction section which acts as a transition piece from circular to rectangular cross section is of reinforced concrete construction. Contraction ratio is 10.4 to 1 in a length of 30 feet (9.14 m).

Diffusion takes place immediately downstream of the test section in a concrete diffuser which also returns the flow to a circular section. The horizontal expansion angle is 1.43 degrees and the vertical 3.38 degrees in an overall length of 46.5 feet (14.17 m).

A 12.5 foot (3.81 m) diameter, four-blade Curtiss Electric propeller driven at 900 RPM by a 1250 KVA synchronous electric motor provides the air flow in the wind tunnel. Any desired test section dynamic pressure between zero and 100 pounds per square foot (0 - 4.79 kPa) can be obtained by proper blade pitch angle positioning.

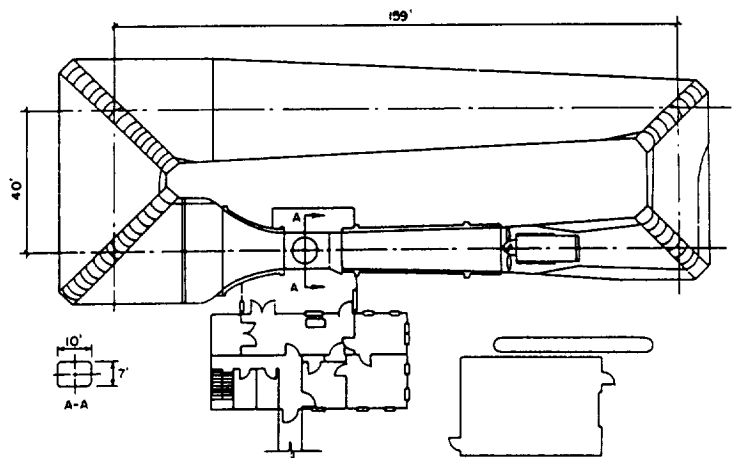


Figure 1 - TAMU-LSWT facility diagram

Three separate studies were performed on tunnel parameters critical to the testing of a two-dimensional laminar flow airfoil in preparation for the investigation of the SM701. These studies examined the test section freestream turbulence intensity, the floor and ceiling boundary layers,

and the external balance system accuracy and repeatability.

Freestream turbulence intensity measurements were made at five different locations in the test section using a single component TSI hotwire and associated equipment. The data was not filtered or linearized, therefore the worst case is presented. Data was taken at each location in the test section at 10 different dynamic pressures. Each data point was obtained by analyzing 2048 samples acquired at 2000 Hz. Figure 2 presents a plot of turbulence intensity vs. dynamic pressure for each location. The turbulence intensity does not vary significantly with location but is a strong function of dynamic pressure. The SM701 airfoil was tested in the low turbulence intensity range of 4 psf (191 Pa) to 24 psf (1.15 kPa) dynamic pressure. The turbulence intensity ranges from approximately 0.3% to 0.9% in this range.

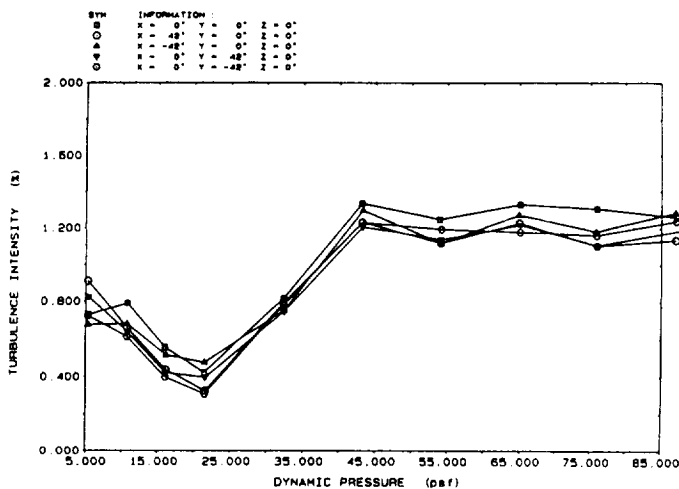


Figure 2 - Freestream turbulence intensity

The test section floor and ceiling boundary layers were measured by using a twelve port boundary layer rake. The rake facilitated the measurement of the eleven total and one static pressures by the PSI-8400 pressure measurement system. The top total pressure port was located 3.60 inches (91.4 mm) above the surface and the static pressure port was located 4.10 inches (104.1 mm) above the surface. The boundary layer thickness was measured at the SM701 leading edge, quarter chord, and trailing edge locations as well as seven other locations on both the floor and the ceiling at ten different dynamic pressures. The displacement, momentum, and energy thicknesses were calculated based on the boundary layer surveys at each location. The

boundary layer thicknesses on the floor and the ceiling were nearly identical. The boundary layer thickness, defined as the height above the surface where the local velocity reached 95% of the freestream velocity, grew from approximately 1.10 inches (28 mm) at the entrance to the test section to 2.55 inches (68 mm) at a point 42 inches (1.07 m) behind the center. The boundary layer thickness ranged from 1.85 inches (47 mm) at the leading edge location to 2.10 inches (53 mm) at the trailing edge location at a dynamic pressure of 30 psf (1.44 kPa).

The facility's six component pyramidal external balance was checked for repeatability and accuracy by repeatedly loading a single component with calibrated precision weights. These tests were done with both the tunnel drive motor off and on. The drag measurements were repeatedly accurate to within 0.05 lbs. (0.22 N) and the lift measurements were accurate to within 0.10 lbs. (0.44 N). Both components were slightly better behaved with the drive motor on rather than off. It is believed this is due to the vibrations present in the system from the motor eliminating any sticking in the mechanical components of the balance system.

#### MODEL DESCRIPTION:

The SM701 airfoil is a 16 percent thick, laminar flow airfoil designed for high maximum lift and low profile drag while exhibiting docile stall characteristics. The model constructed for this test had a span of 6.97 ft (2.17 m), a chord of 2.68 ft (0.82 m) and an area of 18.66 ft<sup>2</sup> (1.734 m<sup>2</sup>).

The model was built around an existing metal wing which was used as the backbone for the SM701 model. Foam was sanded to match the shape of the upper and lower surfaces of the existing wing and then glued to the wing with an epoxy resin. Templates were generated on a computer and cut out of aluminum plates. These templates were mounted to each end of the foam covered wing. The foam was sanded down to the templates and covered with multiple layers of fiberglass. The final shape was obtained by using Bondo Body Filler to smooth out any irregularities in the airfoil shape. The model was sanded to a smooth finish and painted. After painting, the wing was polished by wet sanding with 600 grit sandpaper. Outer templates were then made from the model by using oversized

profile shapes and filling in the gaps between the templates and the model with Bondo. From these templates, actual cross-sections were taken from three different stations along the span of the model. When compared with plots of the theoretical coordinates, some differences were noticed between the actual shape of the model and the theoretical shape. On the lower surface near the trailing edge, an error in thickness of 0.35% of the chord was observed between the two shapes. On the upper surface at approximately 5% from the leading edge, a maximum error of 0.28% was observed again in the thickness. In both cases, the model was thicker than the theoretical shape (Figure 3).

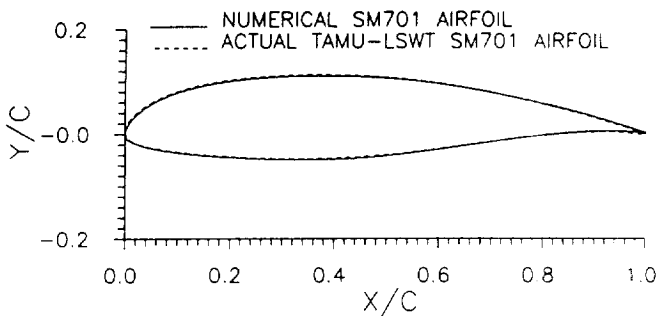


Figure 3 - Comparison of numerical and actual airfoil shape

A steel mounting plate was attached to the model at one end and this plate was then bolted to the external balance. There was a 0.125 inch (3.12 mm) gap at the test section ceiling and the model extended into the floor. A floorplate with a 0.125 inch (3.12 mm) gap around the model was used.

Under high aerodynamic loadings the model was observed to contact the floorplate so the gap was enlarged. This, however, allowed air from the balance room to be drawn into the test section and adversely affect the airflow around the model. Several floorplate configurations which attempted to eliminate this flow were tested and efforts were also made to close the model-ceiling gap. The final configuration that was tested is shown in Figure 4. A 0.125 inch (3.12 mm) ceiling gap was used to prevent interference during yaw sweeps. The bottom of the wing was placed 0.3125 inches (8 mm) above the floor and a spacer was placed between the model and the mounting plate with the floorplate fitting around the spacer. This configuration

redirected any airflow from underneath the test section parallel to the floor.

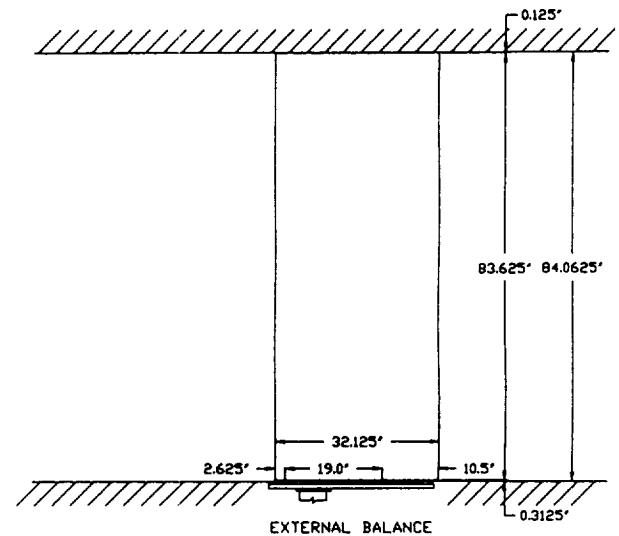


Figure 4 - Line drawing of airfoil in TAMU-LSWT test section

#### TEST CONDITIONS:

Angle of attack sweeps were run on the SM701 airfoil at four different dynamic pressures. Six component external balance data was taken at angles of attack from negative stall through positive stall in one degree increments. The set dynamic pressures were 4 psf (191.5 Pa), 9 psf (430.9 Pa), 15 psf (718.2 Pa), and 24 psf (1.149 kPa); these correspond to Reynolds Numbers of  $1 \times 10^6$ ,  $1.5 \times 10^6$ ,  $2.0 \times 10^6$ , and  $2.5 \times 10^6$ . The minimum Reynolds Number was limited by the ability to set and maintain a constant dynamic pressure in the test section. The maximum Reynolds Number was limited by the wind loads imposed on the external balance system.

Standard two-dimensional buoyancy, solid blockage, and wake blockage corrections as described in Reference 5 were applied to the force and moment data.

Drag on the SM701 was also measured by the momentum loss method. A traversing mechanism was installed in the tunnel which held a seven-hole pressure probe. The probe tip was located one chord length behind the trailing edge of the airfoil. The total pressure was then read at 51 points in a 5 inch (127 mm) wide sweep using the PSI-8400 pressure measurement system. These 51 pressures were then integrated to obtain



the section drag coefficient of the airfoil. The momentum loss method is very time consuming and was therefore run only on select cases. It was used to measure the laminar drag bucket of the airfoil. The particular cases run were:  $-4^\circ$ ,  $-2^\circ$ ,  $0^\circ$ , and  $3^\circ$  angle of attack at  $1.0 \times 10^6$ ,  $1.5 \times 10^6$ , and  $2.0 \times 10^6$  Reynolds Numbers, and  $-5^\circ$  through  $6^\circ$  in  $1^\circ$  increments at a Reynolds Number of  $2.5 \times 10^6$ .

Extensive flow visualization was also performed on the SM701. The method used was fluorescent oil painted on the surface of the airfoil. The test section was then bathed in ultraviolet light to show the contrast in the oil flow. The flow visualization was used to see laminar separation bubbles, transition, separation, flow angularity, and surface imperfections as well as examining the flow at the airfoil/floor and airfoil/ceiling junctures.

## TEST RESULTS:

### VARIATION WITH REYNOLDS NUMBER

The lift coefficient and pitching moment coefficient were plotted versus angle of attack (Figures 5 and 6) showing the effects of Reynolds Number. These effects are small throughout the majority of the curve. They tend to be larger near stall. Near stall the lift coefficient increased with Reynolds Number. The maximum lift coefficient increased 1.54% between  $1.0 \times 10^6$  and  $2.5 \times 10^6$  Reynolds Number.

The lift coefficient was also plotted versus both the balance drag coefficient data and the momentum loss method drag coefficient data (Figures 7 and 8). The drag coefficient measured by both methods is the lowest at the high Reynolds Number.

### RESULTS AT 2.5 MILLION REYNOLDS NUMBER

The values for lift coefficient, both forms of drag coefficient, and pitching moment coefficient are presented along with the numerical predicted data and available experimental data acquired by D. Althaus for the  $2.5 \times 10^6$  Reynolds Number case (Figures 9-11). The balance measured a maximum lift coefficient of 1.53 at an angle of attack of approximately  $15^\circ$ . The measured zero lift angle of attack was about  $-4^\circ$ . The inverted maximum lift coefficient was -

0.637 at  $-10^\circ$ . The data also shows the positive stall to be quite gentle with no sudden or dramatic loss of lift. The inverted stall, however, was measured to be very hard with nearly a 40% drop in lift in just  $1^\circ$ . The pitching moment coefficient was fairly smooth and constant throughout the angle of attack range except at inverted stall. The values ranged from -0.112 at  $-1^\circ$  to -0.074 at  $15^\circ$ . The pitching moment in inverted stall increased rapidly to nearly zero. A laminar drag bucket was measured by both the balance and the momentum loss method. The minimum drag coefficient measured by the balance was 0.0093 at  $-2^\circ$ . The lowest drag part of the bucket was  $3^\circ$  wide while the entire bucket was  $5^\circ$  wide. The momentum loss method measured a minimum drag coefficient of 0.0062 at  $-1^\circ$ .

The transition location was observed at various angles of attack through the use of the fluorescent oil flow visualization. The measured transition locations ranged from 64% aft of the leading edge at  $-2^\circ$  to 12% aft at  $14^\circ$  on the upper surface. At  $-2^\circ$  the transition location on the lower surface was measured to be approximately 60% aft of the leading edge.

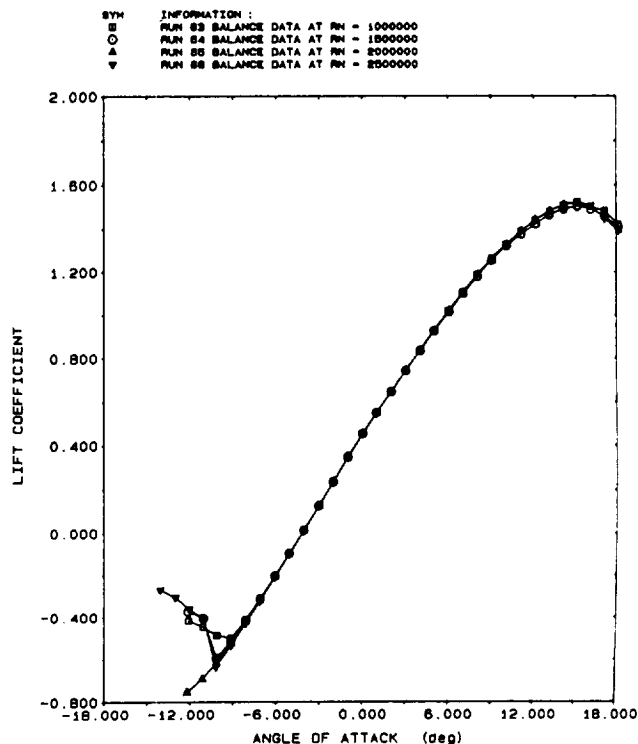


Figure 5 - Reynolds Number effects on lift

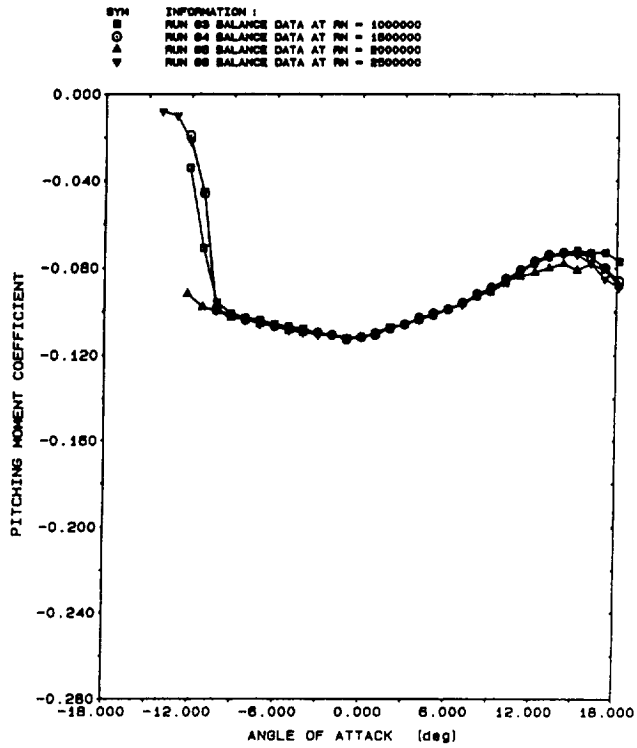


Figure 6 - Reynolds Number effects on pitching moment

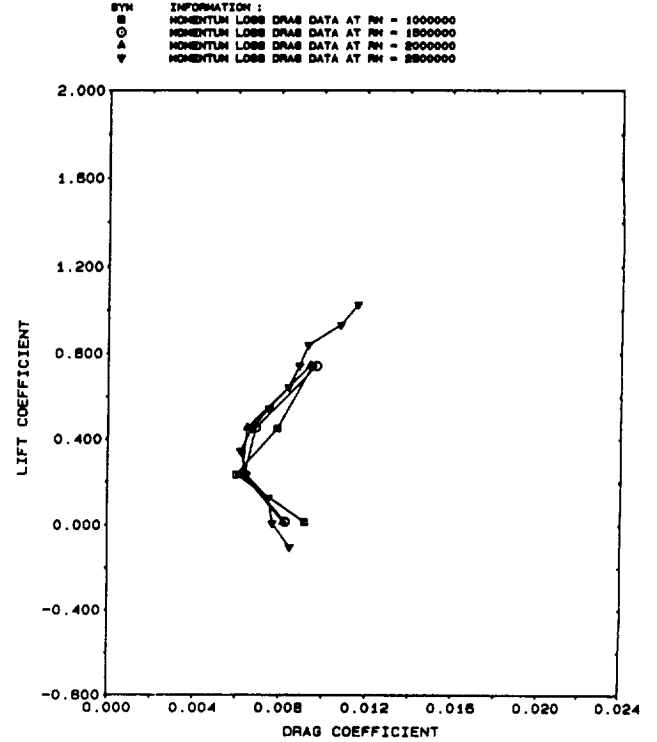


Figure 8 - Reynolds Number effect on momentum loss drag

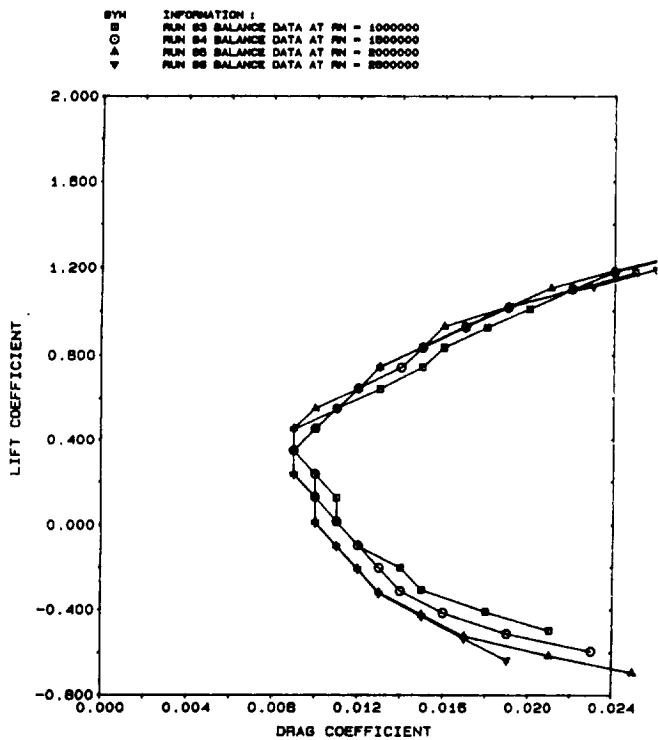


Figure 7 - Reynolds Number effect on balance drag

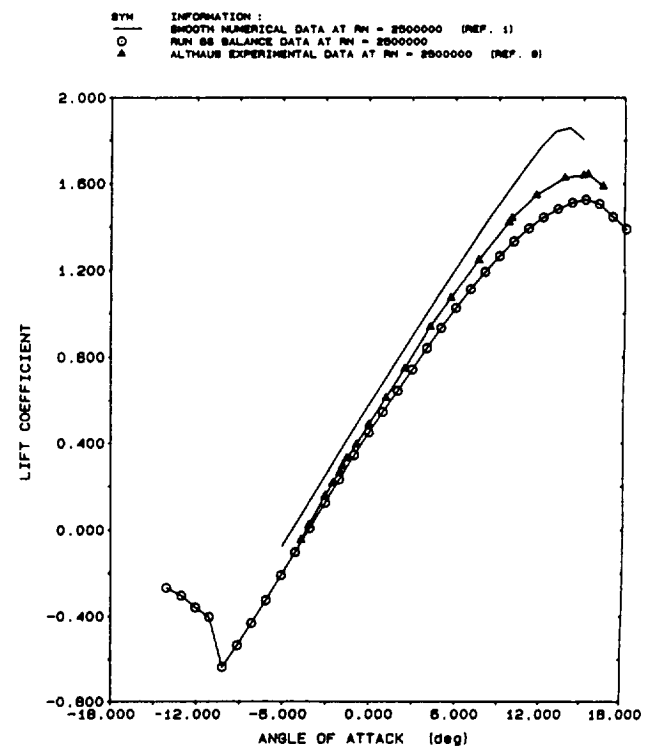


Figure 9 - Lift coefficient comparison

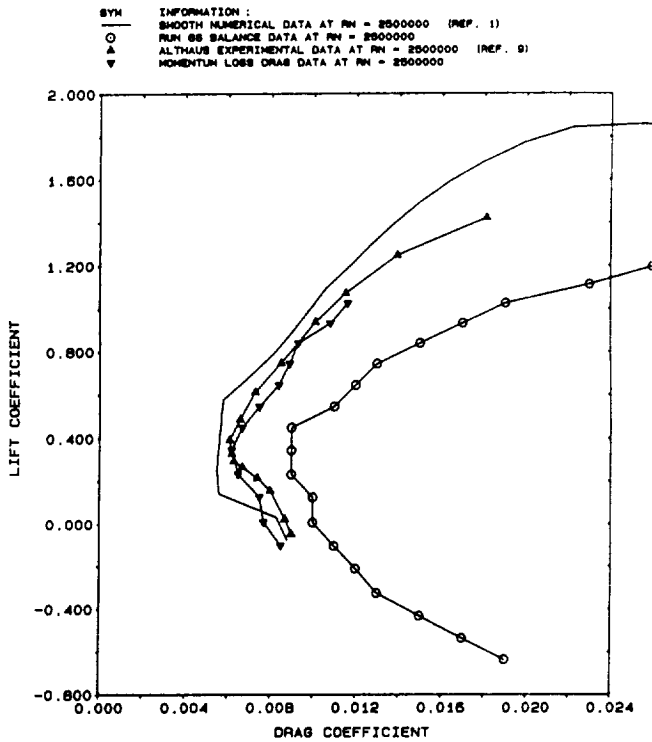


Figure 10 - Drag coefficient comparison

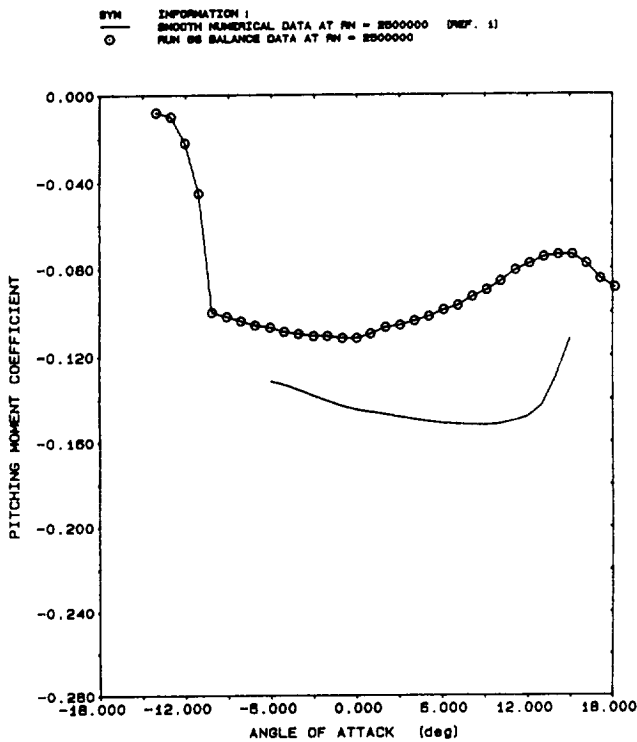


Figure 11 - Pitching moment coefficient comparison

DATA ANALYSIS:

The lift coefficient versus angle of attack curve of the experimental data agrees well with the numerical predicted values through the low  $C_L$  range. The slope tends to flatten somewhat above a lift coefficient of 0.4. The maximum lift coefficient measured was 17% lower than predicted and approximately 7% lower than measured by Althaus. No predicted data was available for the inverted stall condition. The predicted zero lift angle of attack was  $-5.294^\circ$  while the experiment showed this to be approximately  $-4^\circ$ .

The drag coefficient measured by the balance was approximately 35% higher than the predicted and 27% higher than the momentum loss drag values through the laminar drag bucket. The measured balance drag near stall is very much higher than predicted. The momentum loss method drag coefficients were quite close to the predicted values and actually lower at some angles. These measured drag coefficients were extremely close to those measured by Althaus. The momentum loss method is generally a more accurate way to measure the two-dimensional section characteristics of an airfoil.

The pitching moment coefficient as measured by the balance was significantly lower than predicted. In general, the measured moment was about 35% lower.

The observance of the transition location tended to agree very well with the predicted values, especially at higher angle of attack. The observed transition was about 10% forward of the predicted location near  $0^\circ$  angle of attack. The observed and predicted locations agreed within 3% at all other angles of attack.

Investigations were performed to consider possible three-dimensional, boundary layer, and reverse flow effects on the data due to the presence of gaps between the top of the model and the roof and the bottom of the model and the floor.

One effect studied was induced drag due to tip effects. Induced drag was calculated using the standard equation:

$$C_{Di} = C_L^2 / \pi AR$$

This equation assumes complete three-dimensional tip effects even though the gap was small. Induced drag was found for a range of lift coefficients at various Reynolds Numbers and

subtracted from the drag measured during the test. This, however, resulted in negative numbers for drag for a majority of lift coefficients. Therefore, full three-dimensional conditions were not being observed and can not held accountable for the variations between theory and experiment.

As a result of the gap between the top of the model and the roof, skin friction drag on the top of the model was calculated for drag corrections, assuming boundary layer conditions of velocity along the surface. Skin friction drag was calculated using the following equation:

$$C_f = 0.074/RN^{0.2}$$

The local dynamic pressure in the boundary layer of the roof was estimated at 0.25 inch (6.35 mm) from the roof from boundary layer surveys conducted earlier. Using this information, the coefficient of skin friction drag was calculated. Calculations based on this assumption, added to the induced drag calculations, provided a net negative drag at most angles of attack (Figure 12).

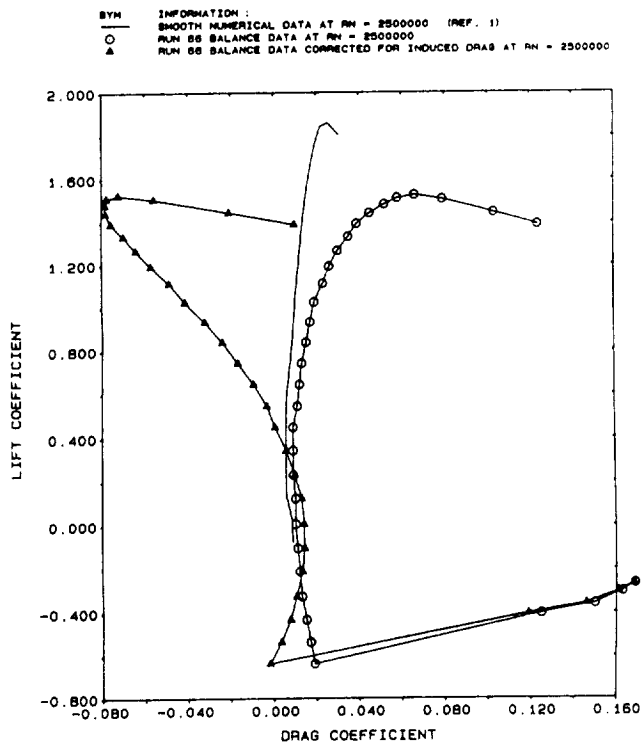


Figure 12 - Induced drag correction comparison

Knowing that floor and ceiling boundary layers interacted with the model, their effects on the model were also studied. Previously

performed boundary layer surveys provided values for the boundary layer thickness which interacted with the model, for both the floor and the ceiling. These thicknesses were weighted against the span of the model. For both the floor and the ceiling, the boundary layer thickness that interacted with the model was between 2% and 3% of the span. Flow visualization indicated that the other 94% to 96% of the model was unaffected by the boundary layer. The local dynamic pressures were found in the floor and ceiling boundary layers and multiplied by their respective weighted thicknesses. The same was done for the mid span of the model that was left unaffected. When these three products were added together, the actual dynamic pressure can adjusted for boundary layer effects. Results of this produced a reduction in dynamic pressure of no more than 2%.

Utilizing the flow visualization photographs, the areas on the wing near the floor and ceiling where separated and reverse flow existed were identified. It was assumed that these areas were not producing lift. The percentage of total effective area loss ranged from 1.94% at 2° angle of attack to 2.56% at 14°. The average loss over the entire angle of attack range was 2.26%.

Incorporating the above changes in the data would have resulted in proportional increases in the coefficients, but these corrections were not applied to the data presented.

#### DISCUSSION AND CONCLUSIONS:

The results of a wind tunnel test on a two-dimensional model of the SM701 airfoil have been reported. Comparisons were made with theoretical calculations and other experimental results obtained earlier. A combination of direct measurements of lift, drag, and pitching moment are presented based on external balance measurements, suitably corrected for wind tunnel blockage and wall effects.

Boundary layer effects were considered and calculations were made to interpret these effects on the balance measurements. It was concluded that these and three-dimensional effects caused by the presence of a one-eighth inch gap between the upper end of the model and the ceiling moderated the values slightly; however, the simplified calculations to predict

three-dimensional effects showed that the test produced results that were nearly two-dimensional. Wake rake data were obtained to survey the drag at low angles of attack where the critical cruise conditions exist. Minimum drag coefficients of about 0.0062 compared with analytically predicted values of about 0.0055, being about 13% higher at the cruise condition. There do appear to be three-dimensional or boundary layer effects in the lift coefficient at high angles of attack. The maximum lift coefficient measured was approximately 17% lower than calculations predicted. The shape of the lift curve suggests some three-dimensional effects may have been present. The performance above stall indicates that the design goal of gentle stall characteristics was met.

Flow visualization techniques allowed the determination of transition from both the upper and lower surfaces at several Reynolds Numbers and angles of attack. These observations indicated that laminar flow was achieved over about 64% of the upper surface and 60% of the lower surface at  $-2^\circ$  angle of attack and  $2.5 \times 10^6$  Reynolds Number, closely approximating the predicated values.

The negative pitching moment of -0.100 is approximately 35% less than the predicted value. The zero lift angle of attack was about  $1.3^\circ$  higher than predicted.

Measured values of stall lift coefficient at negative angles showed the  $C_L$  to be about -0.6 for three Reynolds Number cases. At a Reynolds Number of two million a negative lift coefficient of -0.77 was measured.

Together, all the experimental results obtained tend to verify the trends determined by analytical predictions. Because of the size of the model, there is greater confidence in the measurements at Reynolds Numbers of two million and above. These experimental data, combined with those reported in Reference 9 tend to support the expected performance of the airfoil as predicted by its designers.

#### REFERENCES:

1. Somers, Dan M.; and Maughmer, Mark D.: The SM701 Airfoil. Airfoils Incorporated, State College, Pennsylvania, 1990.
2. Morelli, Piero: The "World Class" Glider Design Competition. FAI Announcement. Technical Specifications, November, 1990.
3. Low Speed Wind Tunnel Facility Handbook. Texas A&M University, College Station, Texas, 1985.
4. Schlichting, Hermann: Boundary-Layer Theory. McGraw-Hill Book Company, New York, 1979.
5. Rae, William H.; and Pope, Alan: Low Speed Wind Tunnel Testing. John Wiley and Sons, New York, 1984.
6. Eppler, Richard: Airfoil Design and Data. Springer-Verlag, Berlin, 1990.
7. Hoerner, Sighard F.: Fluid-Dynamic Drag. Hoerner Fluid Dynamics, New Mexico, 1965.
8. Riley, Donald R.: Wind-Tunnel Investigation and Analysis of the Effects of End Plates on the Aerodynamic Characteristics of an Unswept Wing. NACA TN-2440, 1951.
9. Althaus, D.; and Wurz, W.: Wind Tunnel Tests of the SM701 Airfoil. Universitat Stuttgart, 1991.
10. Abbott, Ira H.; Von Doenhoff, Albert E.; and Stivers, Louis S., Jr.: Summary of Airfoil Data. NACA Rep. 824, 1945.

**VERIFICATION OF THE SM701 AIRFOIL AERODYNAMIC  
CHARACTERISTICS UTILIZING THEORETICAL TECHNIQUES**

Kenneth D. Korkan  
Robert C. Griffiths  
Stefan A. Uellenberg  
Texas A&M University  
Aerospace Engineering Department  
College Station, Texas 77843-3141

Presented at the OSTIV Congress,  
Uvalde, Texas, August 1991

NASA Grant Number NAG1-1260-FDP

# VERIFICATION OF THE SM701 AIRFOIL AERODYNAMIC CHARACTERISTICS UTILIZING THEORETICAL TECHNIQUES\*

Kenneth D. Korkan\*\*  
Robert C. Griffiths\*\*\*  
Stefan A. Uellenberg\*\*\*\*  
Texas A&M University  
Aerospace Engineering Department  
College Station, Texas 77843-3141

## Abstract

Utilizing a state of the art low speed airfoil design/analysis methodology, the *Airfoil Program System*, (APS), the SM701 laminar flow airfoil was designed specifically for the World Class sailplane by Airfoils, Incorporated. The airfoil was expected to exhibit certain design criteria as predicted by the computational methodology, e.g. docile stall characteristics, high maximum lift with low profile drag and restrained pitching moment. Verification of these characteristics was performed by testing a two-dimensional SM701 airfoil in the Texas A&M University Low Speed Wind Tunnel (TAMU-LSWT) and comparing the theoretical predictions with the experimental results. Comparisons of the results were done implementing graphical output of  $c_l$  vs  $c_d$ ,  $c_l$  vs  $\alpha$ , and  $c_m$  vs  $\alpha$ . Further limited comparisons were done with respect to transition location on the airfoil, utilizing flow visualization techniques in the wind tunnel. These transition locations are predicted in the airfoil analysis methodology utilized in this study. The problem of airfoil roughness is also addressed by the (APS). While roughness in the form of grit was not added to the wind tunnel model, predicted theoretical roughness values were included in the test comparisons.

## Nomenclature

$c$	Chord Length
$c_l$	Lift Coefficient
$c_{l_{max}}$	Maximum Lift Coefficient
$c_d$	Drag Coefficient

---

\*This research has been supported by NASA Langley RC Grant 1-1260-FDP.

\*\* Professor; \*\*\*Undergraduate Research Assistant; \*\*\*\*Graduate Research Assistant.

$c_m$	Pitching Moment Coefficient
$c_{m_{c/4}}$	Pitching Moment Coefficient; Quarter-Chord
$H_n$	Shape Factor
$r$	Roughness factor
$p$	Static Pressure
Re	Reynolds Number
$u(x, y)$	Tangential Vel. Component in Boundary Layer
$U(x)$	Potential-Flow Velocity
V	Velocity
$x/c$	Horizontal Airfoil Coordinates
$x_{cr}/c$	Critical Transition Location
$y/c$	Vertical Airfoil Coordinates
$\alpha$	Angle of Attack
$\alpha_{L_0}$	Angle of Zero Lift
$\delta_1(x)$	Displacement Thickness
$\delta_2(x)$	Momentum Thickness
$\delta_3(x)$	Energy Thickness

## I. Introduction

The formulation of an accurate, computational, low speed airfoil analysis methodology has been attempted by theoreticians for more than 30 years. The creation of such an analysis would mean savings in money as well as lives due to the decreased need for extensive flight testing. The first step in determining the validity of such a methodology resides in verification through experimental techniques, such as the use of wind tunnels.

One such methodology that attempts airfoil analysis at low speeds is known as the *Airfoil Program System* (APS), created by Dr. Richard Eppler of the University of Stuttgart. This approach utilizes a panelling method as well as semi-empirical data and an integral boundary layer method<sup>1</sup>. Upon specification of the airfoil coordinates, Reynolds number and angle of attack, the computer analysis calculates velocity and pressure distributions, lift, drag and moment coefficients, and addresses transition and separation locations. The APS methodology also allows the inclusion of different roughness factors for the airfoil to simulate rain, insects, etc. The system is also capable of designing airfoils for specific purposes, such as the airfoil of interest to this study, designated the SM701.

The SM701 laminar flow airfoil was designed for the World Class sailplane utilizing the (APS) methodology as developed by Eppler and modified by Mr. Dan Somers of Airfoils, Inc. The design team, consisting of Mr. Somers and Dr. Maughmer of Penn State University, had the goal of achieving specific aerodynamic performance objectives,



e.g. high maximum lift and low profile drag with restrained pitching moment in addition to docile stall characteristics<sup>2</sup>.

Verification of the results as predicted by Somers and Maughmer was to be tested by constructing an exact duplicate of the theoretical airfoil, installing the airfoil in the TAMU-LSWT, and testing under the same conditions utilized by Airfoils, Inc. in the APS computer analysis. Due to structural construction limitations, the final airfoil shape was slightly different from the exact SM701, as seen in Figure 1. Important differences were observed between the theoretical SM701 airfoil ("Airfoil 1"), and the SM701 airfoil constructed at Texas A&M University ("Airfoil 2"). Airfoil 2 displayed a finite thickness at the trailing edge; Airfoil 1 had a sharp trailing edge. Also, due to some structural differences toward the leading edge, a camber alteration was also expected. The maximum measurable difference between the two airfoils was limited to  $0.35\%c$ , according to Nicks. Therefore, to obtain a valid comparison between the experimental and theoretical data, it became necessary to determine the new airfoil coordinates. These coordinates were then used to execute the computational analysis and obtain a valid comparison to the wind tunnel results.

The method utilized to obtain the new airfoil coordinates included cutting a template of the airfoil cross section, followed by a digitizing procedure whereupon the airfoil coordinates were determined by computational methods. These new points were non-dimensionalized, smoothed and re-integrated with the *Airfoil Program System*. These new results were then compared with the wind tunnel test data to produce a valid comparison.

The aerodynamic coefficients of interest in this study included lift coefficient, drag coefficient, and moment coefficient about the quarter chord. Other characteristics of concern were transition location, maximum lift coefficient, and Reynolds number effects on the coefficients. Special interest was given to differences between the theoretical and experimental results, as well as verifying the desired SM701 airfoil performance objectives.

## II. Computational Theory

The (APS) methodology employs the potential-flow analysis method which utilizes panels with distributed surface singularities. The singularities used are parabolically distributed vortices, placed along each panel, and the flow condition requires the tangential velocity component to equal zero along the body surface. The shape of each panel is determined by a polynomial of the third degree, fixed in a local coordinate system. The Kutta condition must also be satisfied at the trailing edge singularity. If the trailing edge has zero thickness, then the airfoil analysis replaces the trailing edge shape with a new one having a zero degree trailing edge, and none of the airfoil coordinates are changed. If the trailing edge has a finite thickness, the APS methodology switches to a different solution which simulates a wake behind the trailing edge.

For the boundary layer calculations, the pressure gradient  $dp/ds$  is necessary, where  $s$  is the arc length along the airfoil surface. Positive  $dV/ds$  means a favorable pressure gradient or negative  $dp/ds$ , while a negative  $dV/ds$  implies an adverse pressure gradient. An integral method is used for the analysis of the boundary layer. If  $u(x, y)$  is the tangential velocity component within the boundary layer, then the potential-flow velocity is:

$$U(x) = \lim_{y \rightarrow \infty} u(x, y) \quad (1)$$

the displacement thickness is:

$$\delta_1(x) = \int_0^{\infty} \left( 1 - \frac{u(x, y)}{U(x)} \right) dy \quad (2)$$

the momentum thickness is:

$$\delta_2(x) = \int_0^{\infty} \left( 1 - \frac{u(x, y)}{U(x)} \right) \frac{u(x, y)}{U(x)} dy \quad (3)$$

and the energy thickness is:

$$\delta_3(x) = \int_0^{\infty} \left[ 1 - \left( \frac{u(x, y)}{U(x)} \right)^2 \right] \frac{u(x, y)}{U(x)} dy \quad (4)$$

Then the shape factors are taken as:

$$H_{12} = \frac{\delta_1}{\delta_2} \quad (5)$$

and

$$H_{32} = \frac{\delta_3}{\delta_2} \quad (6)$$

Approximate solutions can then be determined by allowing only velocity distributions of the form:

$$\frac{u}{U} = f\left(\frac{y}{\delta(x)}, H(x)\right), \quad (7)$$

where  $\delta$  is a thickness factor and  $H$  a shape factor. Calculations within the analysis are simplified by realizing that  $H_{32}$  and  $\delta_2$  are functions of  $H_{12}$ ,  $\delta_1$  and  $\delta_3$ . For values of  $H_{32}$  where  $1.51509 < H_{32} < 1.57258$ , the flow region over the airfoil is assumed to have adverse pressure gradients. These constants are derived in a semi-empirical manner utilizing the so-called Hartree profiles<sup>1</sup>. For turbulent boundary layers, separation is assumed to occur at values of  $H_{32} < 1.46$ . More generally, boundary layer separation is assumed to occur at a point where  $\left(\frac{\partial u}{\partial y}\right)_{y=0} = 0$ . This boundary layer process aids in the development of  $C_{l_{max}}$

values, as well as  $C_l$  values beyond  $C_{l_{max}}$ . The flowfield analysis utilized in the (APS) includes results beyond  $C_{l_{max}}$ , or effective angle of attack of close to 20 degrees. For a detailed discussion of the (APS), reference is recommended to Eppler<sup>1</sup>.

### III. Methodology

The testing of the SM701 airfoil was done with an extensive array of parameters necessarily compatible with both the experimental and theoretical investigations. The most important "similarity parameter" was the shape of the airfoil. It was important that the airfoils tested in the tunnel and on the computer were as close to identical as possible, as discussed earlier. A total of five Reynolds numbers were investigated, i.e. 700,000, 1,000,000, 1,500,000, 2,000,000, and 2,500,000. These values fell within the range of capability of the wind tunnel and in the realm of low speed flight for the SM701 airfoil as computationally simulated.

Also, as roughness has a dramatic effect on the performance of a laminar flow airfoil, it was important that the wind tunnel model be as smooth as possible. Also, since the (APS) is capable of simulating roughness, choosing the correct roughness factor used in running the methodology was imperative. To show the large difference between a computationally developed smooth and rough airfoil, graphical data will be presented in Section IV. The SM701 wind tunnel model was not roughed during this study, but preliminary results from a separate wind tunnel/computational comparison study display similar trends<sup>4</sup>. The angle of attack values were also important. The range of  $\alpha$  values were run from beyond negative  $c_{l_{max}}$  through positive  $c_{l_{max}}$ . For the SM701 airfoil, this range was  $-15^\circ$  to  $18^\circ$ .

To assess the accuracy of the APS transition prediction, flow visualization techniques were performed on the SM701 airfoil while in the wind tunnel. This included covering a chordwise portion of the airfoil with oil and observing the flow pattern over the wing with ultraviolet, or "black" lights. The transition point was not difficult to determine from this method. Separation conditions, especially laminar separation bubbles, were also examined during this flow visualization process. However, due to the time consuming nature of this experimental methodology, only a limited number of flow visualization tests were conducted.

In summary, two different disciplines were active during this study, i.e. the experimentalists and the theorists. The experimentalists concentrated on constructing an accurate wind tunnel model and conducting tests in an environment as free from anomalies as possible. They were also responsible for correcting any errors found during the tests. The theoreticians, however, were responsible for recreating a physical environment in a computational methodology. The merging of the two philosophies always produces interesting results.

## IV. Results

The aerodynamic coefficients obtained from the (APS) analysis were compared to the experimental data resulting from wind tunnel research on the SM701 airfoil. Implementing the corrected airfoil coordinates with the computer methodology, similar results were expected between the theoretical and experimental studies of the SM701 airfoil.

### Drag Polar

The APS was consistent in predicting a lower drag coefficient value at higher lift coefficients than that shown from the wind tunnel data. At the same time, the wind tunnel results showed lower  $c_d$ 's at smaller values of  $c_l$ . In other words, the laminar "bucket region", the area of concern for the Olympic-class sailplane, was shifted "downwards" for the wind tunnel data. Figure 2, which displays the drag polar for a Re of 1,000,000, shows this trend for the entire range of Reynolds numbers. Also displayed is the roughed APS results. As expected for the roughed data, the drag coefficient increased and can be seen in Figure 2. Here, in the laminar bucket region where  $c_l = 0.4$ , the predicted  $c_d$  values nearly double between the smooth and rough results. As Re increases to 1,500,000 and 2,500,000 as seen in Figures 3 and 4 respectively, a decrease in  $c_d$  is apparent. This was expected as an increased Re value tends to increase the turbulence of the flow over an airfoil, resulting in the flowfield staying attached to a further aft chordwise location postponing separation. In all five Reynolds number tests, the trends displayed in Figures 2, 3 and 4 are similar. The wind tunnel results fall between the smooth and rough values as predicted by the APS analysis.

The accuracy of the design criterion can be deduced from these three Figures also. According to the designers of the SM701, the  $c_{l_{max}}$  of at least 1.6 should occur at a  $c_d$  value of approximately 0.0240. The curves displayed by the APS smooth airfoil datapoints meets this criteria, while the wind tunnel data shows a  $c_l$  value of approximately 1.05 at a  $c_d$  value of 0.0240. However, both the theoretical and experimental curves display docile stall characteristics as evidenced by the gentle curve in the  $c_{l_{max}}$  region.

### Lift Coefficient vs. Angle of Attack

As shown in Figures 5, 6 and 7, the  $\alpha_{L_0}$  point has shifted between the theoretical to experimental results. The shift is approximately one half of a degree to the positive side for the wind tunnel results. However, the lift curve slope  $\left(\frac{dc_l}{d\alpha}\right)$  is the same for both. The maximum lift coefficient as predicted by the APS was determined from a set of boundary conditions developed empirically by Somers and Maughmer. The  $c_{l_{max}}$  was considered to have occurred when either the  $c_d$  value of the upper surface exceeded 0.024 or if the length of turbulent separation along the upper surface increased beyond the 0.1c location,

as measured from the trailing edge. On Figure 5, the  $c_{l_{max}}$  value for the wind tunnel model was shown to be lower than the smooth theoretical, e.g., from 1.561 to 1.5122. The  $\alpha$ 's at which  $c_{l_{max}}$  occurs in each case are consistent; approximately  $11^\circ$  for the APS calculations and  $15^\circ$  for the wind tunnel results, as displayed in Figures 5-7. Again on Figure 5, the negative  $c_{l_{max}}$  values correspond closely, occurring near  $-10^\circ$  with a  $c_l$  value close to  $-0.5$ . Also in Figures 5,6 and 7, the theoretical with roughness results are also included for comparison analysis. Generally, as shown in all three  $c_l$  vs  $\alpha$  Figures, the only variation from the APS determined values for the smooth and rough data occurred around the positive and negative  $c_{l_{max}}$  values.

As the Reynolds number increases to 1.5 million, (Figure 6) and to 2.5 million, (Figure 7) certain trends become apparent. First, the  $c_{l_{max}}$  values predicted by APS for the smooth airfoil increases from close to 1.7 to near 1.84. The positive  $c_{l_{max}}$  value for the wind tunnel model remained virtually identical. The wind tunnel model did display slightly less docile stall characteristics beyond  $c_{l_{max}}$  for increasing Re. Negative  $c_{l_{max}}$  was shown to exhibit more negative values for increasing Re, as shown again in Figures 5,6 and 7. This trend occurred for both the theoretical and the experimental airfoils. However, while the angle at which negative  $c_{l_{max}}$  occurred for the wind tunnel model remained close to  $-10^\circ$ , negative  $c_{l_{max}}$  for the theoretical airfoil occurred at increasingly negative  $\alpha$  values as Re increased ranging from  $-10^\circ$  in Figure 5 to  $-14^\circ$  in Figure 7. The rough values showed more intolerance to changing Re, remaining between  $-11^\circ$  and  $-12^\circ$  for all five Reynolds numbers.

#### Pitching Moment Coefficient vs. Angle of Attack

The  $c_{m_{c/4}}$  vs  $\alpha$  values showed an insensitivity to changing Reynolds number, as shown in Figures 8,9 and 10. The smooth and rough theoretical values remained very close to each other, never varying by more than 2.5%. The difference between the theoretical and experimental values is larger, but remained constant throughout the range of Reynolds numbers tested. The trends displayed between the theoretical and experimental  $c_m$  are similar, however, as shown in the  $c_m$  vs  $\alpha$  Figures. Both the wind tunnel model and the theoretical airfoil display  $c_m$  values in excess of  $-0.1$ , which is the design criteria specified for the SM701 airfoil. However, the theoretical model at no time, for the five Reynolds numbers tested, exceeded 0.148, while the experimental model never exceeded 0.12. Therefore, the restrained moment criteria was met under both conditions, even though values greater than  $-0.1$  were reached. It was found that the design of the SM701 airfoil with 16 percent thickness and a  $c_{l_{max}}$  of at least 1.6 with acceptably low profile drag coefficients could not be achieved without violating the  $-0.1$  pitching moment coefficient constraint<sup>2</sup>.

## Reynolds Number Effect

There was a Reynolds number effect on the results of this study. As shown in Figure 11, the theoretically acquired drag polar displays a decreasing  $c_d$  value for increasing Re. The same trend is displayed in Figure 12 for the wind tunnel tests. Reynolds number effect was negligible except near positive  $c_{l_{max}}$  and negative  $c_{l_{max}}$ , as shown in Figures 13 and 14 for theoretical and experimental results of  $c_l$  vs  $\alpha$  data. The moment coefficient characteristics were shown to be little affected by changing Re, especially at negative and small positive  $\alpha$ 's. This is shown in Figure 15 for the theoretical airfoil and in Figure 16 for the experimental SM701. Angles of attack above 5 degrees display a slight influence by Reynolds number. Figure 17 shows the effect Re had on  $c_{l_{max}}$  values. The wind tunnel data shows little effect, while the roughed theoretical values display an increase in  $c_{l_{max}}$  with an increase in Re. The smooth data shows an even greater change with increasing Reynolds number.

## Transition

The flow visualization technique employed on the SM701 airfoil was successful in showing transition location over the airfoil at different angles of attack. However, due to time constraints, data was only compiled on a single Reynolds number run, which included an angle sweep from  $-2^\circ$  to  $18^\circ$ . Increasingly negative angles of attack were unnecessary as the upper surface of the wing was observed, not the lower. Also, the upper surface at positive angles of attack is the more realistic flight profile for a sailplane, especially during a landing approach. At the higher angles of attack, stall characteristics could be observed on the upper surface of the wing, in particular transition and separation. The experimental transition locations observed at a Reynolds number of 2,500,000 was compared to the transition locations predicted by the *Airfoil Program System*, as shown in Figure 18. This Figure shows transition location from the leading edge of the airfoil in percent chord versus lift coefficient at a constant Re of 2,500,000. The rough results show transition occurring the closest to the leading edge of the airfoil, as can be expected. The experimental results diverge from the theoretical smooth data at approximately 20% from the leading edge location, reconverging at close to the 65% position. This divergence could correspond to a premature tripping of the boundary layer on the wind tunnel model due to roughness, or an inadequacy in the APS analysis. This difference is most pronounced in the  $c_l$  of 0.6 region.

The presence of laminar separation bubbles were impossible to confirm on the airfoil. The importance of laminar separation bubbles cannot be ignored as when they occur, a tremendous amount of drag appears on the wing. Failure to include the effects of these bubbles in drag calculations will cause an underprediction of the  $c_d$  value to occur. The inability to confirm the presence of the laminar separation bubbles could be due to exper-

imental technique and the fact that the bubbles were too short to be positively observed with the human eye.

## V. Conclusions

Verification of the (APS) by experimental methods proved to be largely successful. Theoretical values of  $c_l$ ,  $c_{l_{max}}$  and  $c_{m_{c/4}}$  matched the experimental values and trends. The values predicted for  $c_d$  tended to be less than the experimental values for the "smooth" SM701 airfoil, often by a factor of two or more. This could be attributed to the failure of the APS to consistently predict proper transition and separation locations. The failure to predict any laminar separation bubbles on the upper or lower surfaces is probably not realistic under actual flight or wind tunnel experimentation, therefore resulting in an underprediction of drag coefficient.

The docile stall characteristics exhibited by the airfoil near  $c_{l_{max}}$  could be attributable to the elimination of large laminar separation bubbles on the upper surface. This would also explain their absence during the flow visualization experiments. A docile stall was exhibited in both the theoretical and the experimental results. Low drag was experienced by both airfoils, i.e.,  $c_d$  was close to the design requirement of 0.024 at  $c_{l_{max}}$ . The maximum lift coefficient was satisfied for the APS predictions, but underpredicted by the wind tunnel experiments. Restrained pitching moment characteristics were shown to occur during both experiments. Not surprisingly, the APS predictions are closer to the airfoil design specifications than the wind tunnel results.

A cause for discrepancy between the experimental and theoretical values would lie in the impossibility of producing the exact coordinates of the slightly modified experimental airfoil for theoretical experimentation. Any difference between the coordinate data sets would cause varying results. Boundary layer effects from the walls of the wind tunnel, a floor "suction" and three-dimensional effects caused by gaps in the test section floor and ceiling, and other experimental anomalies would also create random differences in the test results. Even with the errors and discrepancies, the overall results suggest great promise with the (APS) as a valid low speed airfoil analysis system.

## VI. Acknowledgements

The authors would like to thank the crew at the Texas A&M Low Speed wind tunnel, especially Mr. Oran Nicks and Mr. Jorge Martinez, for their cooperation and expertise.

## References

1. Eppler, R. "Airfoil Program System. User's Guide." R. Eppler, c. 1990.
2. Somers, D. M. and Maughmer, M. D. "The SM701 Airfoil." Airfoils, Inc., December 1990.

3. Nicks, O., Steen, G., Heffner, M. and Bauer, D. "Wind Tunnel Investigation and Analysis of the SM701 Airfoil." NAG1-1260-FDP, Presented at the XXII OSTIV Congress, Uvalde, Texas, July 1991.
4. Griffiths, R.C. "Study of Theoretical and Wind Tunnel Results on Flight Performance Degradation due to Ice Accretion." To be published Fall, 1991.
5. Abbott, I.H. and Von Doenhoff, A.E., *Theory of Wing Sections*, Dover Publications, New York, 1959.
6. Schlichting, H., *Boundary Layer Theory*. McGraw-Hill Book Company, New York, 1979.



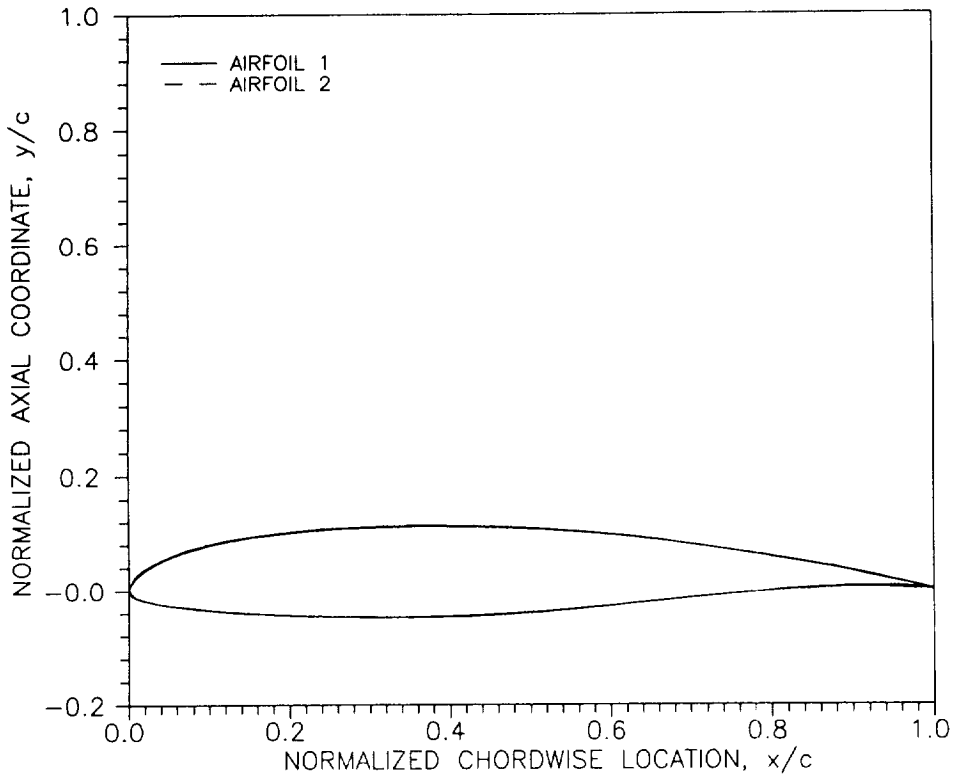


FIGURE 1: COMPARISON OF THE DESIGNED AND ACTUAL CONSTRUCTED SM-701 AIRFOIL

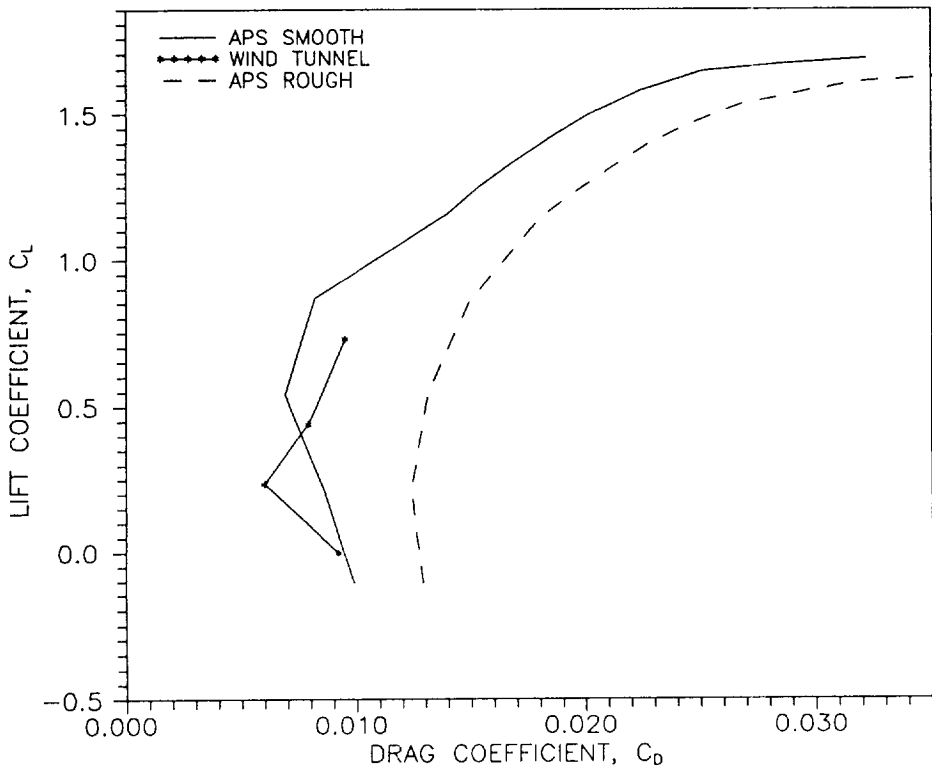


FIGURE 2: COMPLETE DRAG POLAR OF SM701 AIRFOIL AT  $Re = 1000000$

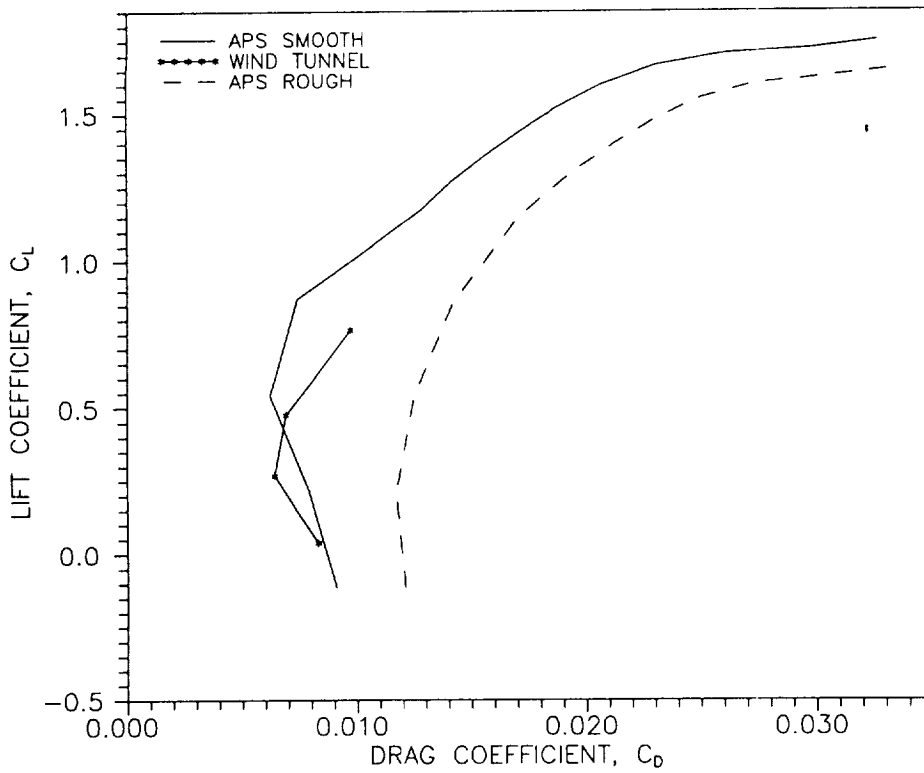


FIGURE 3: COMPLETE DRAG POLAR OF SM701 AIRFOIL AT  $Re = 1500000$

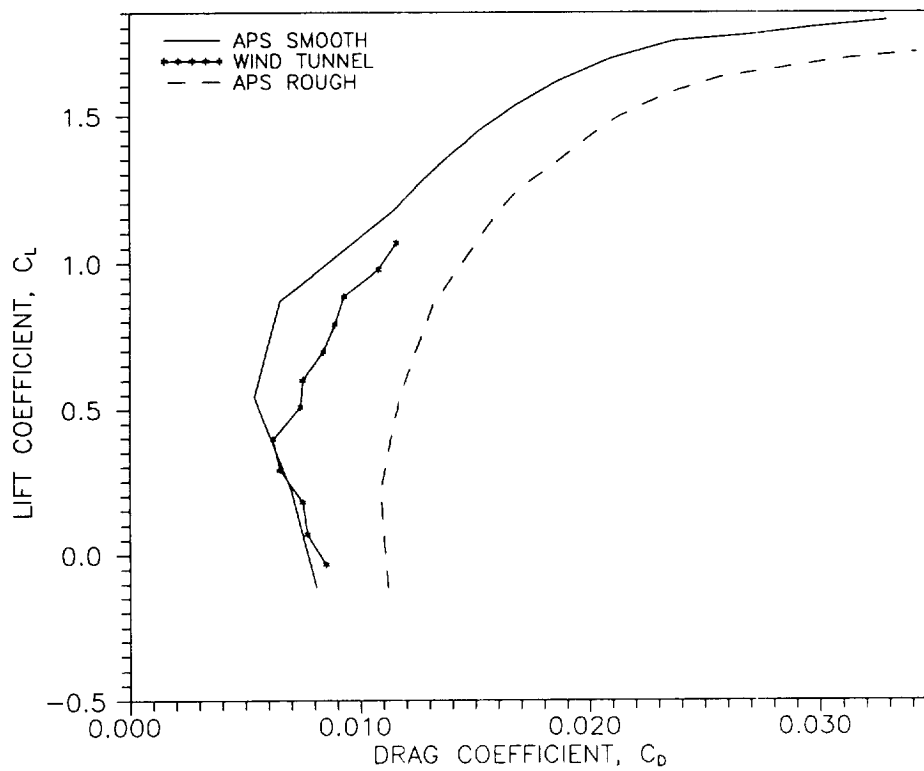


FIGURE 4: COMPLETE DRAG POLAR OF SM701 AIRFOIL AT  $Re = 2500000$

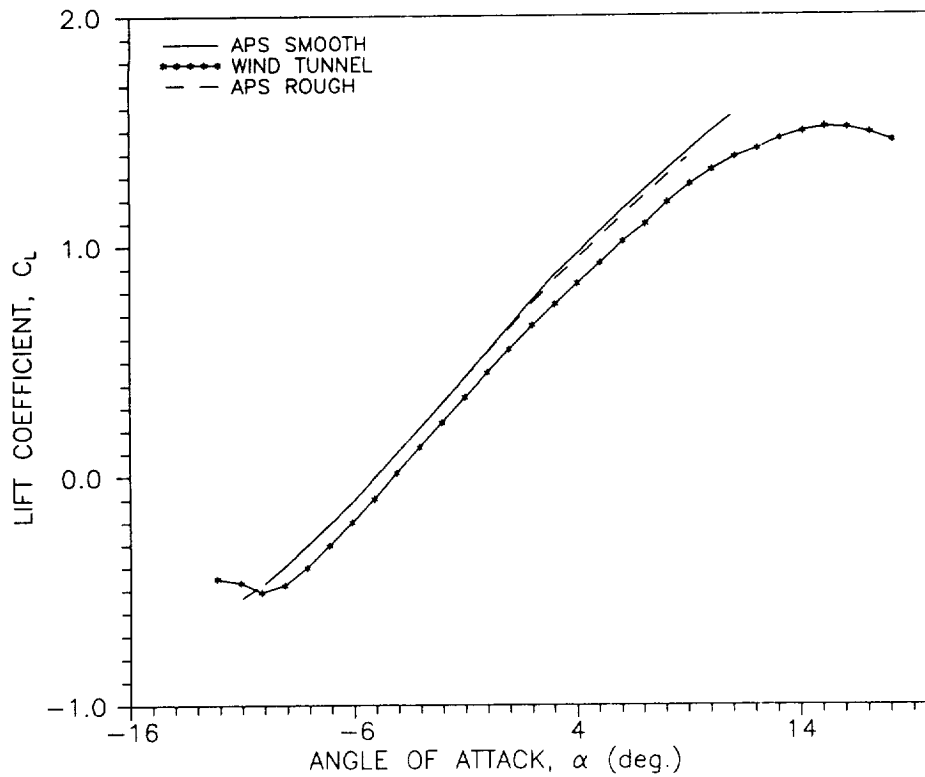


FIGURE 5: COMPARISON OF APS METHODOLOGY TO WIND TUNNEL RESULTS OF THE SM701 AIRFOIL AT  $Re = 700000$

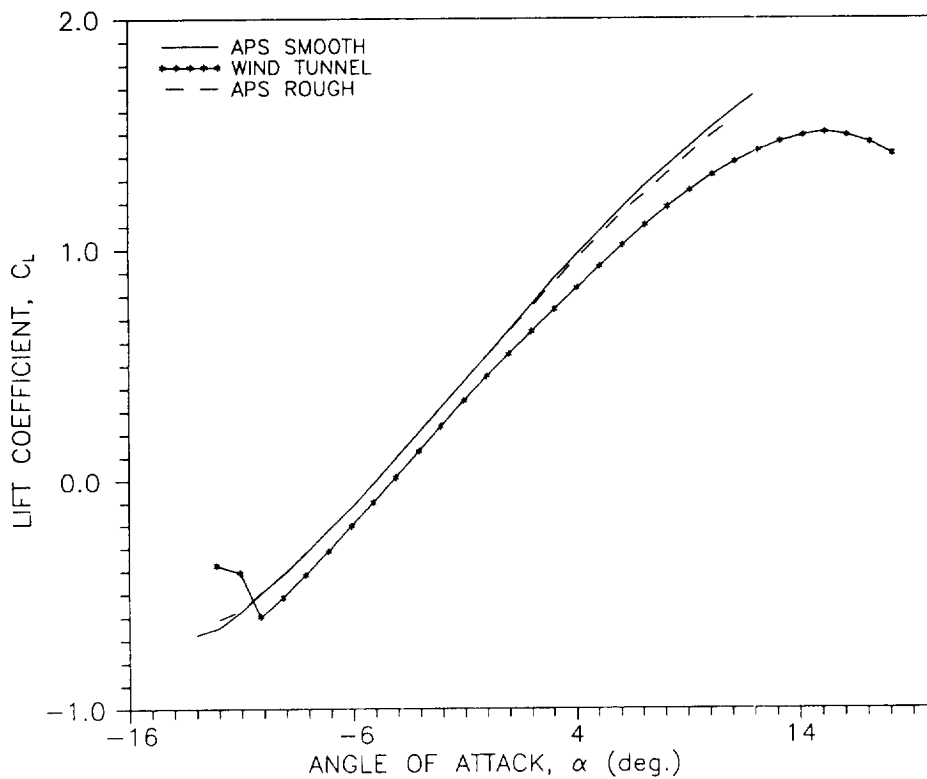


FIGURE 6: COMPARISON OF APS METHODOLOGY TO WIND TUNNEL RESULTS OF THE SM701 AIRFOIL AT  $Re = 1500000$

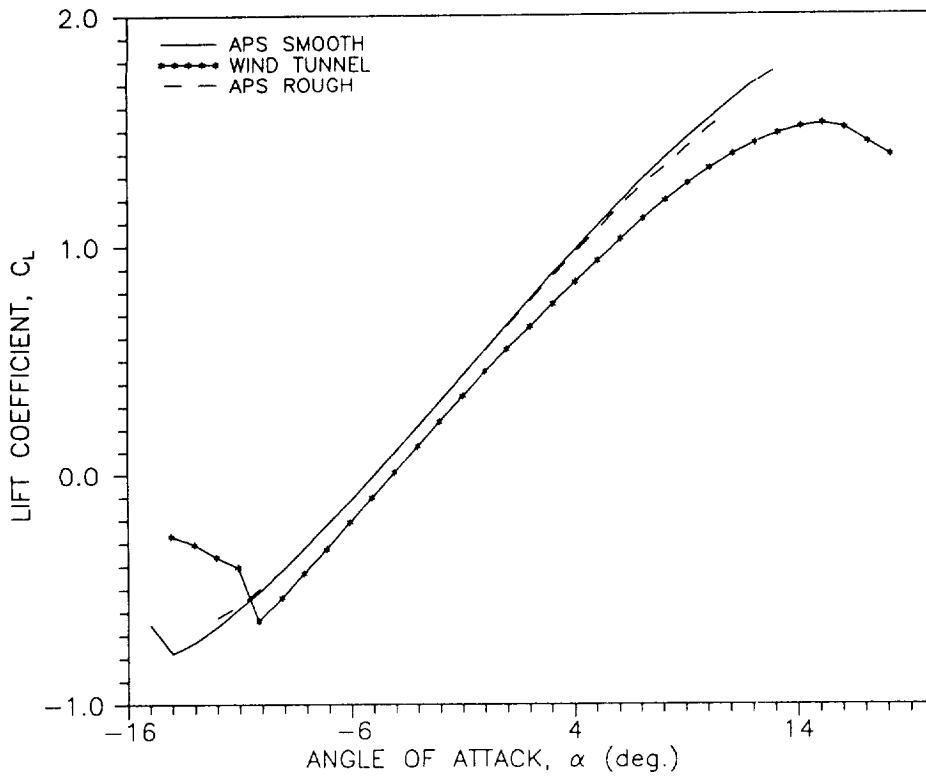


FIGURE 7: COMPARISON OF APS METHODOLOGY TO WIND TUNNEL RESULTS OF THE SM701 AIRFOIL AT  $Re = 2500000$

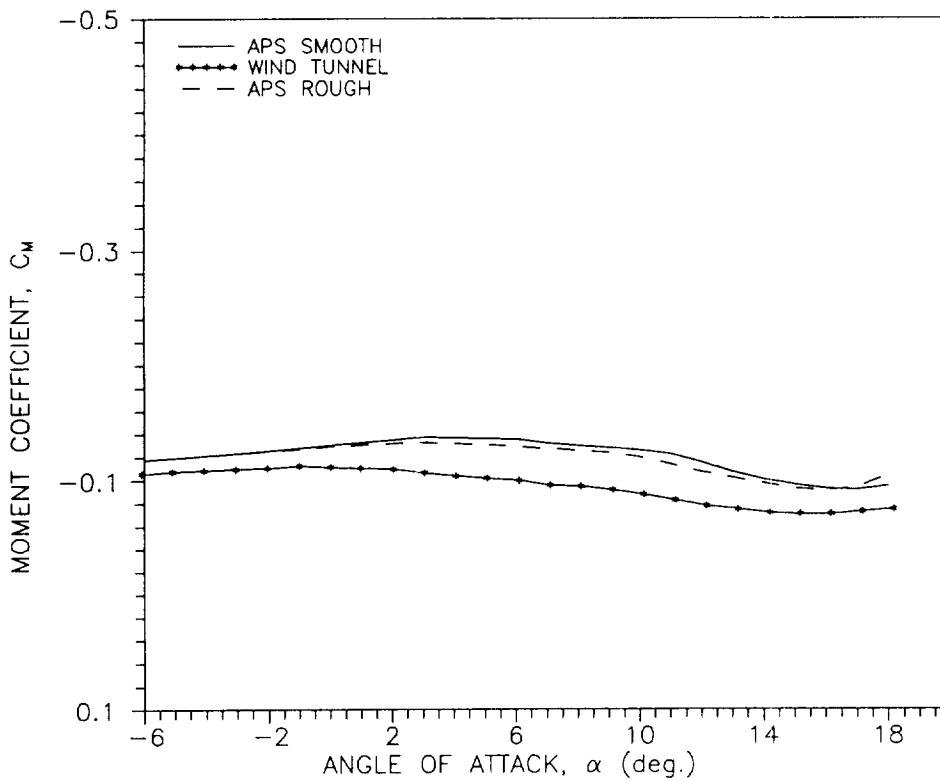


FIGURE 8 : COMPARISON OF APS METHODOLOGY TO WIND TUNNEL RESULTS OF THE SM701 AIRFOIL AT  $Re = 700000$

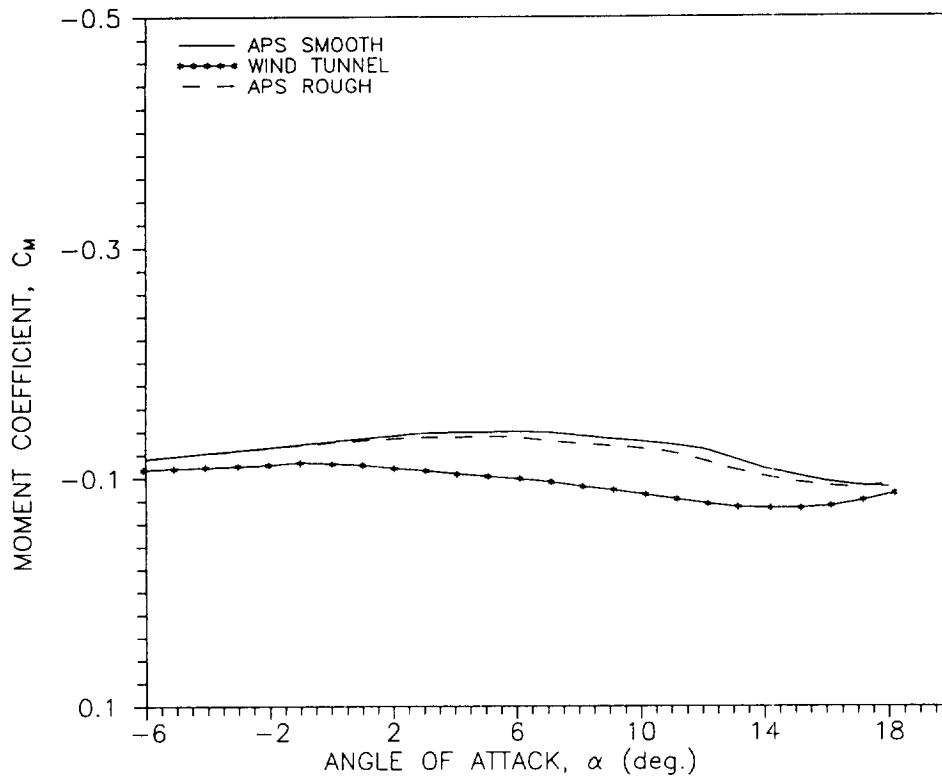


FIGURE 9: COMPARISON OF APS METHODOLOGY TO WIND TUNNEL RESULTS OF THE SM701 AIRFOIL AT  $Re = 1500000$

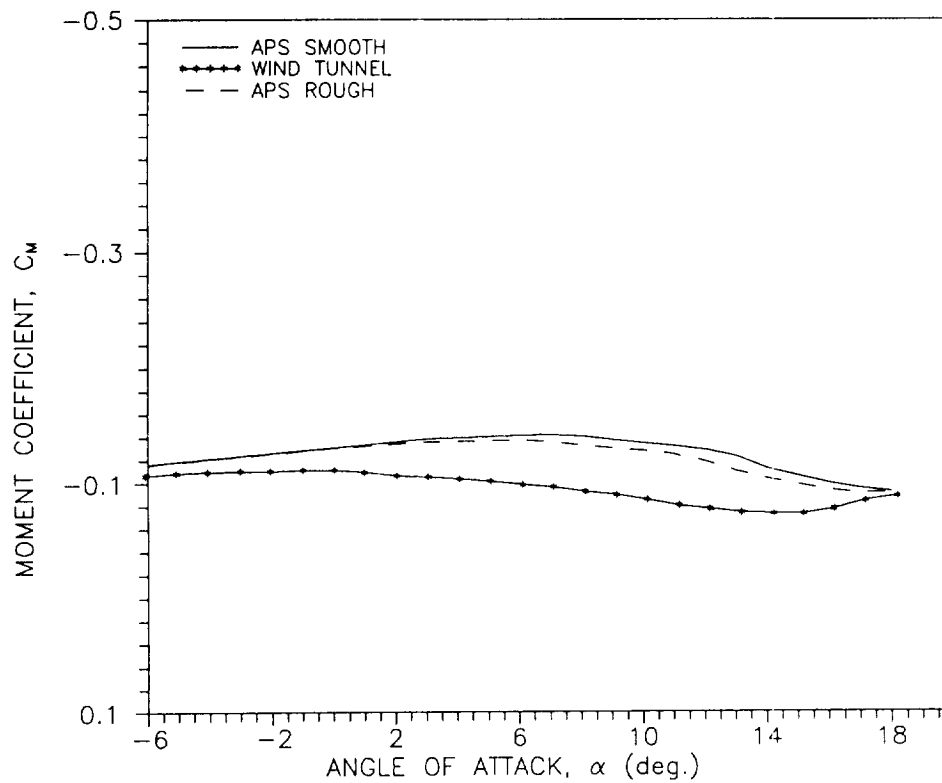


FIGURE 10: COMPARISON OF APS METHODOLOGY TO WIND TUNNEL RESULTS OF THE SM701 AIRFOIL AT  $Re = 2500000$

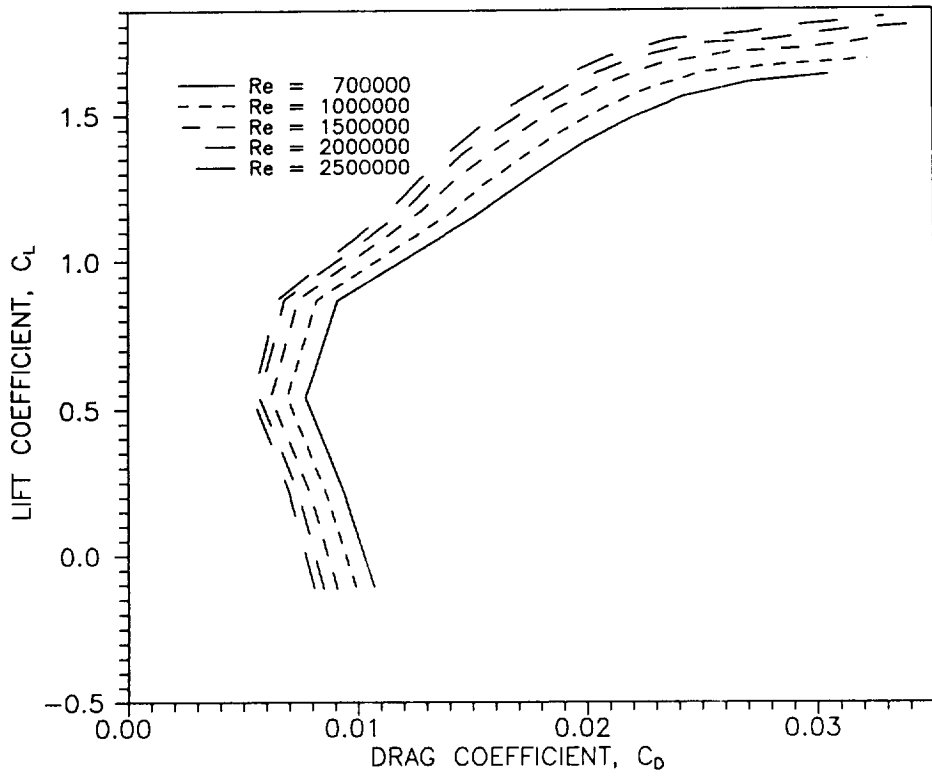


FIGURE 11: THEORETICALLY ACQUIRED DRAG POLARS  
SMOOTH SM701 AIRFOIL AT VARIOUS REYNOLDS NUMBERS

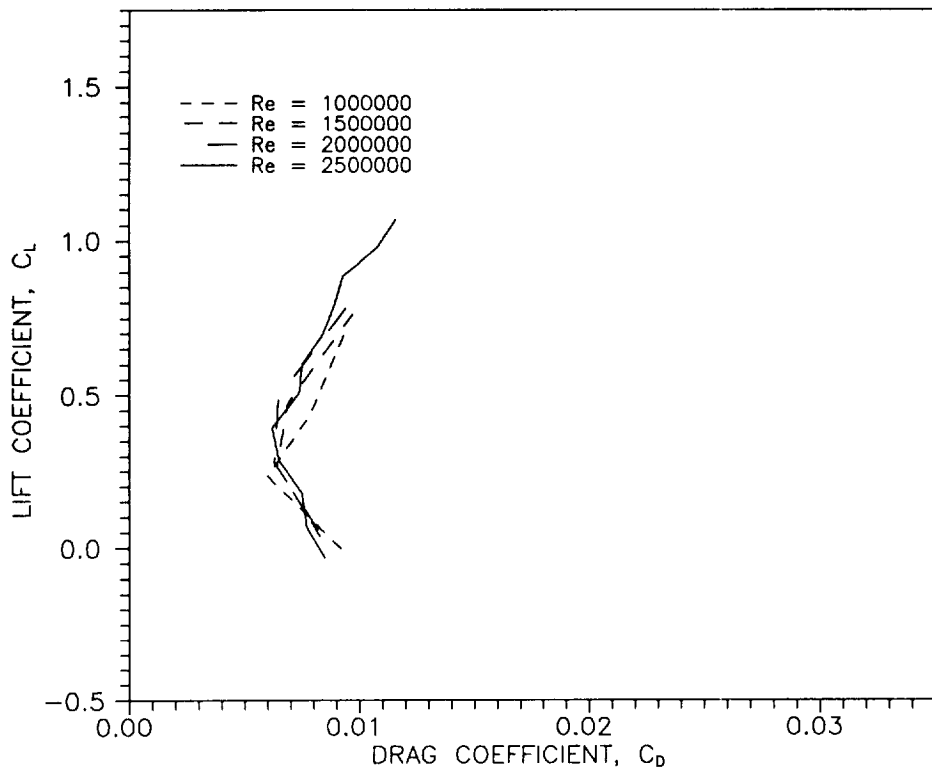


FIGURE 12: EXPERIMENTALLY ACQUIRED DRAG POLARS  
OF THE SM701 AIRFOIL AT VARIOUS REYNOLDS NUMBERS

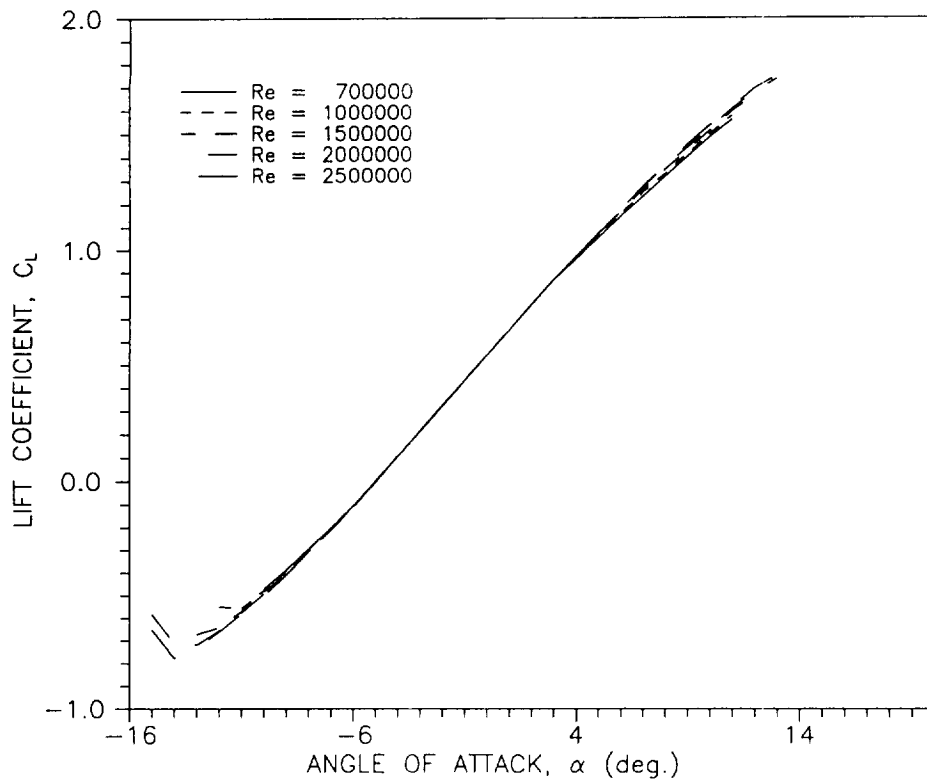


FIGURE 13: THEORETICALLY ACQUIRED LIFT CHARACTERISTICS OF THE SMOOTH SM701 AIRFOIL AT VARIOUS REYNOLDS NUMBERS

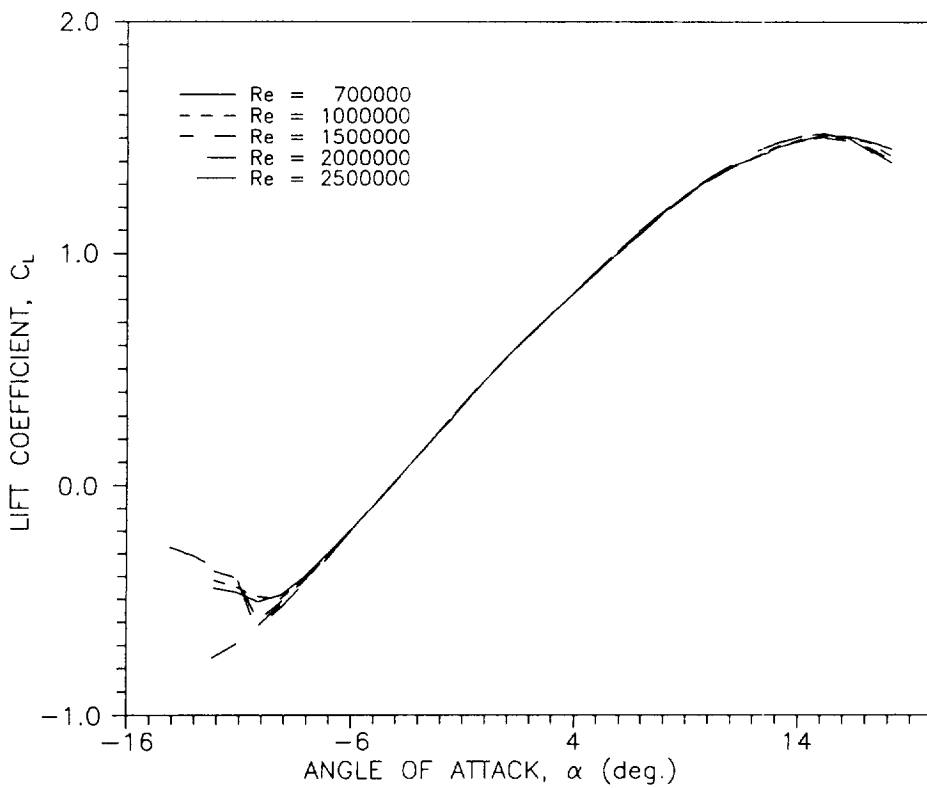


FIGURE 14: EXPERIMENTALLY ACQUIRED LIFT CHARACTERISTICS OF THE SMOOTH SM701 AIRFOIL AT VARIOUS REYNOLDS NUMBERS

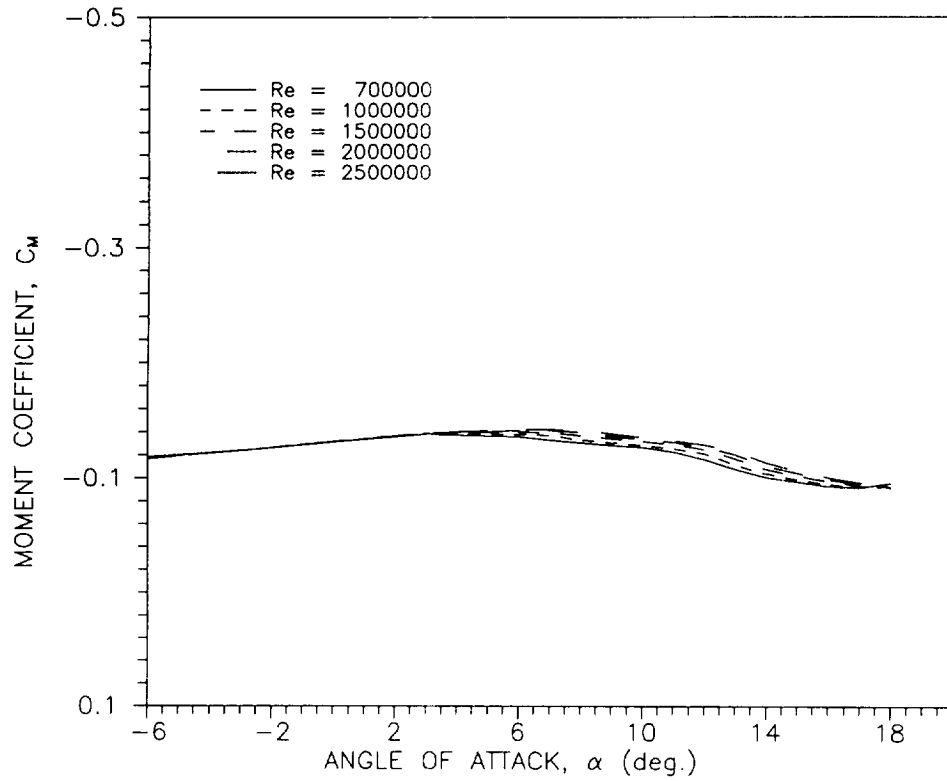


FIGURE 15: THEORETICALLY ACQUIRED MOMENT CHARACTERISTICS OF THE SMOOTH SM701 AIRFOIL AT VARIOUS REYNOLDS NUMBERS

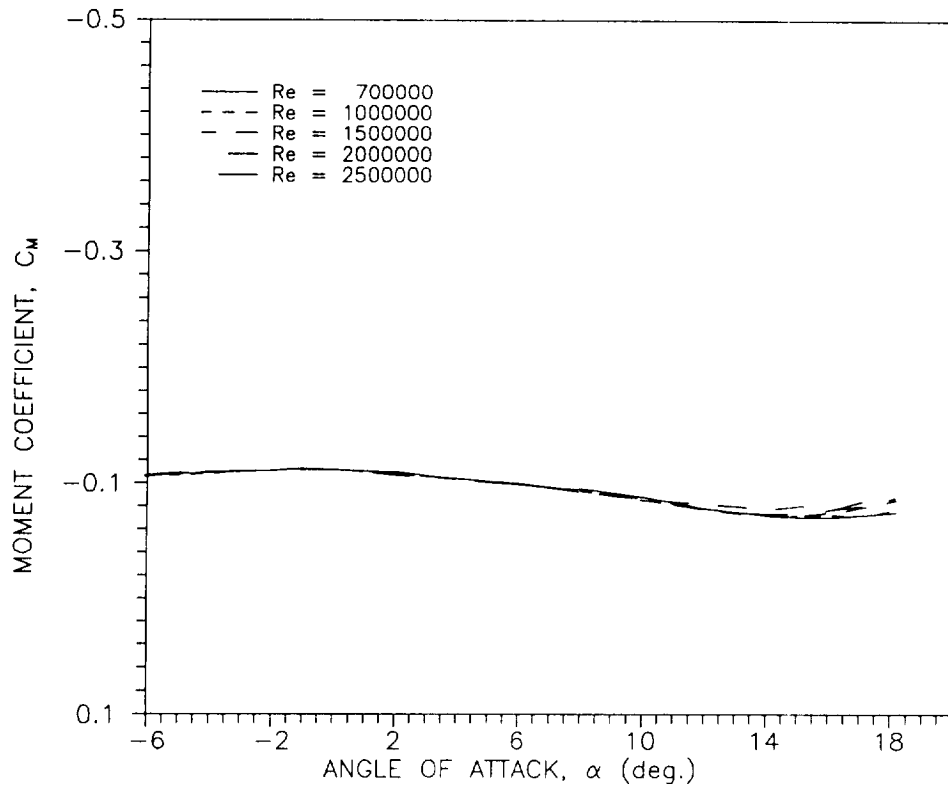


FIGURE 16: WIND TUNNEL ACQUIRED MOMENT CHARACTERISTICS OF THE SMOOTH SM701 AIRFOIL AT VARIOUS REYNOLDS NUMBERS



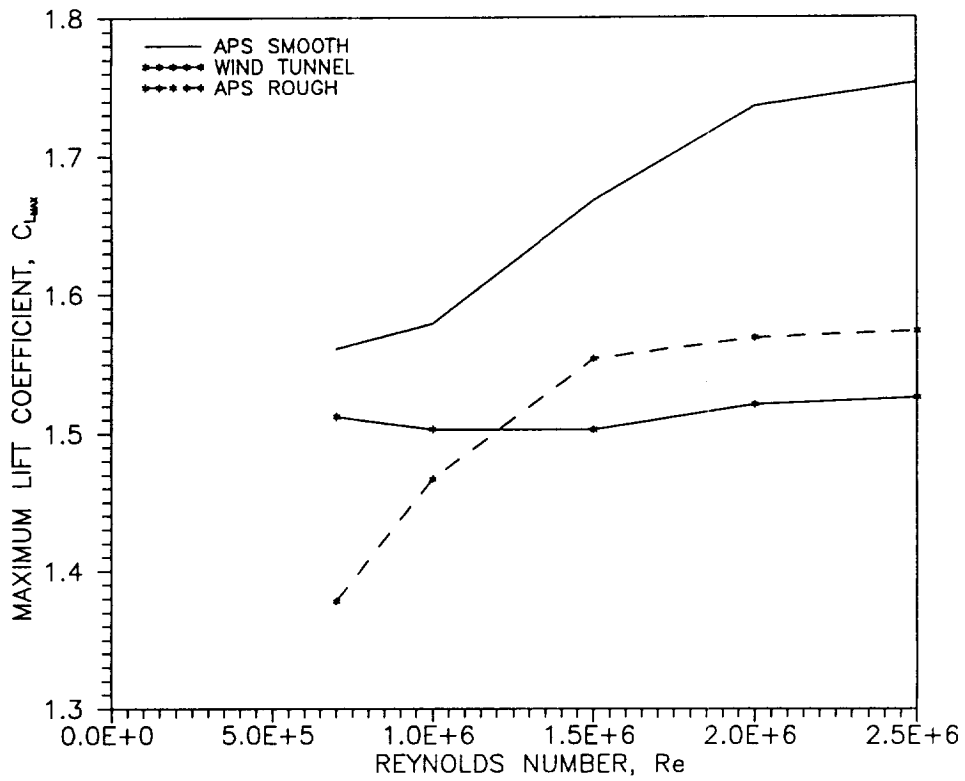


FIGURE 17 :COMPARISON OF REYNOLDS NUMBER EFFECT ON THE MAXIMUM LIFT COEFFICIENT OF THE SM701 AIRFOIL

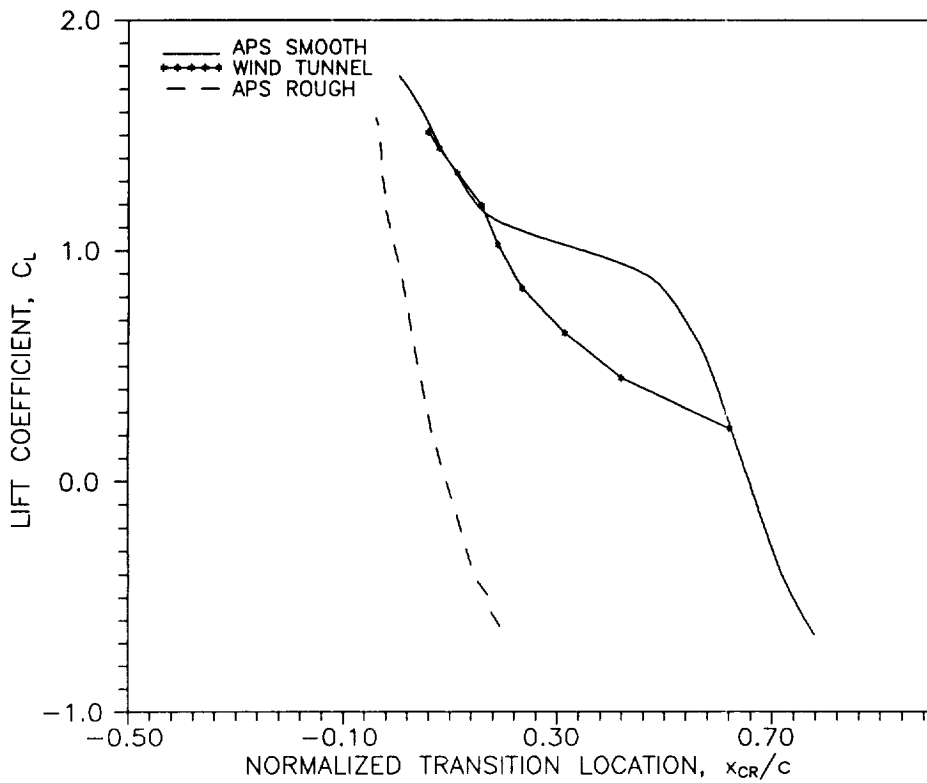


FIGURE 18:COMPARISON OF TRANSITION LOCATION ON THE UPPER SURFACE OF THE SM701 AIRFOIL AT  $Re = 250000$